

BioRadiations

A Resource for Life Science Research

PATH TO DISCOVERY

ProteoMiner™ Protein Enrichment System Technology

In this issue:

Low-Volume DNA Amplification Using the C1000™ Thermal Cycler

Extending Gene Silencing Using siLentMer™ siRNAs

Measuring RNA Integrity Automatically With Experion™ System RQI Feature

Using the Bio-Plex® System to Measure Caspase-1-Dependent Cytokine Secretion

BIO-RAD



Check Out Our Library

Transfecting primary cells? Transforming bacteria? Do you have a protocol for stem cells? Do you need a protocol for rice? Browse our Gene Transfer Protocols library or submit your own protocol.

You can browse and submit:

- Electroporation protocols obtained with the cuvette-based Gene Pulser Xcell™ or plate-based Gene Pulser MXcell™ electroporation systems or Gene Pulser® electroporation buffer
- Lipid protocols for the following transfection reagents: TransFectin™ reagent, a general-purpose lipid; HEKfectin™ or COSfectin™ reagents, both cell line-specific lipids; or siLentFect™ reagent, an RNAi-specific lipid
- Biolistic protocols obtained with the Helios® Gene Gun or PDS-1000/He™ systems

Share your favorite gene transfer methods with Bio-Rad and receive a complimentary gift! For more information, visit us on the Web at www.bio-rad.com/genetransferprotocols/.



Bio-Rad's Gene Transfer Technologies

Biolistic technology is covered by patents owned by Pfizer Inc. The technology is exclusively licensed to Bio-Rad Laboratories, Inc.

Australia 61-2-9914-2800
Austria 43-1-877-89-01
Belgium 32-9-385-55-11
Brazil 55-21-3237-9400
Canada 905-364-3435
China 86-21-6426-0808
Czech Republic 420-241-430-532
Denmark 45-44-52-10-00
Finland 358-9-804-22-00
France 33-1-47-95-69-65
Germany 49-89-31884-0
Greece 30-210-777-4396
Hong Kong 852-2-789-3300
Hungary 36-1-455-8800
India 91-124-402-9300
Israel 03-963-6050
Italy 39-02-216091
Japan 81-3-6361-7000
Korea 82-2-3473-4460
Mexico 52-555-488-7670
The Netherlands 31-318-540666
New Zealand 0508-805-500
Norway 47-23-38-41-30
Poland 48-22-331-99-99
Portugal 351-21-472-7700
Russia 7-495-721-14-04
Singapore 65-6415-3188
South Africa 27-861-246-723
Spain 34-91-590-5200
Sweden 46-8-555-12700
Switzerland 41-61-717-9555
Taiwan 88-62-2578-7189
Thailand 662-651-8311
United Kingdom 44-20-8328-2000
USA Toll free 1-800-4BIORAD
(1-800-424-6723)

discover.bio-rad.com

On the cover:
Conceptual illustration by
Rafael Arroyo and Diana Kollanyi



BioRadiations magazine is published by
Bio-Rad Laboratories, Inc.
2000 Alfred Nobel Drive
Hercules, CA 94547 USA

© 2008 Bio-Rad Laboratories, Inc.
Copyright reverts to individual
authors upon publication.
Reprographic copying for personal
use is allowed, provided credit is
given to Bio-Rad Laboratories.

If you have comments or suggestions
regarding *BioRadiations*, please email
us at bioradiations@bio-rad.com.

BioRadiations

issue 126, 2008

TO OUR READERS

As more and more genomics questions are resolved, there seem to be an inversely proportionate amount of questions and challenges that emerge related to the study of proteomics. One such key challenge is the difficulty characterizing and indentifying proteins in biological samples, because the most prevalent proteins (those that comprise >90%) tend to mask those that are in the minority. ProteoMiner™ protein enrichment system technology was developed to address the need to reduce the presence of high-abundance while enriching low-abundance proteins, making it possible to discover a vast number of proteins with potential roles in disease pathology. In this issue, we interviewed scientists around the world to determine how the ProteoMiner system is making an impact on furthering the discovery of protein biomarkers for a variety of diseases and disorders.

COVER STORY

- 16 ProteoMiner™ Protein Enrichment System Technology Goes Global**
Shawn Miller and Kate Smith, Bio-Rad Laboratories, Inc., Hercules, CA USA

DEPARTMENTS

- 2 What's New**
6 Product Focus
28 Tips and Techniques
30 Solutions*
32 New Literature

TECHNICAL REPORTS

- 11 Low-Volume Amplification of DNA Using the C1000™ Thermal Cycler**
Daniel E Sullivan, Bio-Rad Laboratories, Inc., Hercules, CA USA
- 14 Molecular Weight Estimation Using Precision Plus Protein™ WesternC™ Standards on Criterion™ Tris-HCl and Criterion™ XT Bis-Tris Gels**
Lily Lai, Nik Chmiel, Michael Urban, Tim Wehr, John Walker, and Jeff Xu,
Bio-Rad Laboratories, Inc., Hercules, CA USA
- 22 RNA Quality Indicator: A New Measure of RNA Integrity Reported by the Experion™ Automated Electrophoresis System**
Jeff Gingrich, Bio-Rad Laboratories, Inc., Hercules, CA USA
- 25 Measurement of Caspase-1-Dependent Cytokine Secretion Using the Bio-Plex® Human Cytokine 27-Plex Panel**
Martin Keller and Hans-Dietmar Beer,
Institute of Cell Biology, Department of Biology, ETH Zurich, Switzerland

* A new addition to *BioRadiations*, the Solutions column highlights how researchers have overcome challenges using Bio-Rad products or services.

Legal Notices — See page 32.

Gene Transfer Protocol Library — An Essential Resource For Successful Transfection

The Gene Transfer Protocol library is now located on the Gene Expression Gateway at www.bio-rad.com/genetransferprotocols/. Because a good protocol is essential for successful transfection, we have collected over 300 protocols — obtained from published literature, developed by Bio-Rad scientists, and submitted by customers — to create the Gene Transfer Protocol library.

To access the protocol library, visit the Gene Expression Gateway (www.bio-rad.com/genetransferprotocols/); you will be taken to the Gene Transfer Protocol homepage.

Under the Browse Protocols section select the type of protocol you are interested in — Electroprotocols, Lipid Protocols, or Biolistic Protocols.

Electroprotocols —

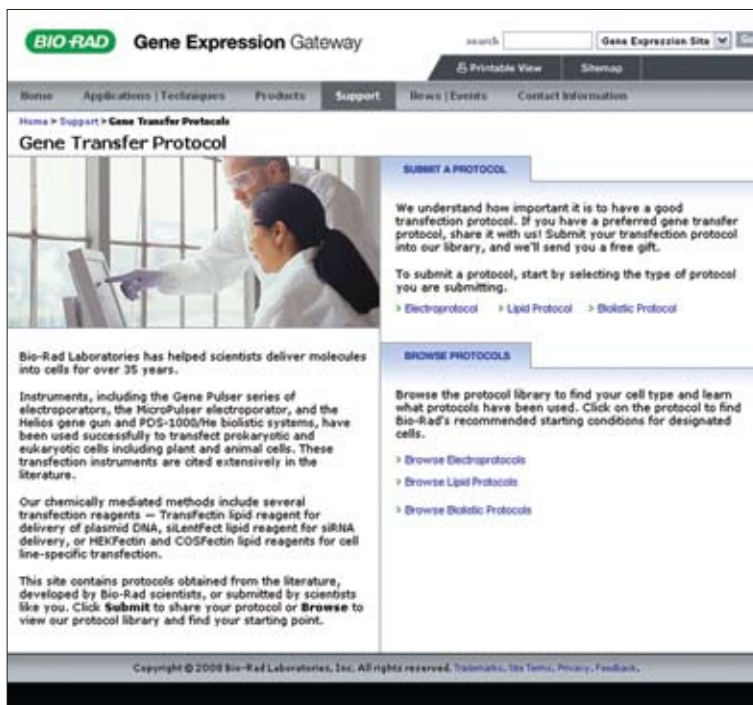
Browse the library by cell type or cell line and learn about the protocols listed. This is a good starting point for your electroporation experiments.

Lipid protocols — Browse the Transfection Reagent References list in the Lipid Transfection section of our website.

Biolistic protocols — Browse the Biolistic Protocols list in the Biolistic Particle Delivery section of our website.

Submit a protocol — You can submit a protocol to any of these lists by either emailing an attached text file or completing the submission form (available on the site in pdf format) and returning by fax or mail. There is a different protocol submission form for each protocol type. Upload your protocol and we will send you a free gift; for every 25 protocols submitted you will be entered into a grand prize drawing (visit www.bio-rad.com/genetransferprotocols/ for complete terms and conditions).

With the Gene Transfer Protocol library, you now have an invaluable resource for quickly identifying a gene transfer protocol. We will be updating the library regularly as we receive new protocols — send your protocol submissions to protocolsubmissions@bio-rad.com.



Bio-Plex Pro™ Wash Stations

The Bio-Plex Pro wash stations eliminate the need to use vacuum manifolds for wash steps in Bio-Plex® assays; simply place the plate in the system and run the wash protocol. Preprogrammed protocols deliver consistent results for any user. The Bio-Plex Pro wash stations make performing Bio-Plex assays as simple as running an ELISA. Benefits include:

- Improved lab productivity
- Reliable and reproducible results
- Optimized onboard protocols
- Two models to meet your needs



Representative results using the Bio-Plex Precision Pro™ human cytokine assay. Experiments determining intra- and inter-assay variability were carried out using the magnetic plate carrier on the Bio-Plex Pro wash station. Intra-assay variability was calculated from triplicate experiments. Inter-assay variability was determined from three separate experiments performed on different days.

Human Target	Mean Observed Concentration, pg/ml	Standard Deviation	%CV
Intra-Assay Variability			
IL-1β	6.39	0.17	2.63
IL-4	13.22	0.59	4.50
IL-6	465.09	13.63	2.93
IL-12 (p70)	10.12	1.14	11.29
IFN-γ	25.03	0.86	3.45
TNF-α	11.84	0.78	6.63
Inter-Assay Variability			
IL-1β	6.23	0.40	6.45
IL-4	16.68	0.21	1.28
IL-6	467.62	17.12	3.66
IL-12 (p70)	16.34	1.51	9.26
IFN-γ	32.40	2.30	7.11
TNF-α	13.91	0.22	1.56

Specifications

Magnetic field	4,500 ± 200 gauss
Vacuum range*	–50 to –150 mbar
Number of dispensing channels	8
Residual volume magnetic wash	<4 µl
Dispensing accuracy	≤2%
Dispensing uniformity	CV ≤4% over the plate
Dimensions (W x D x H)	28 x 37 x 18 cm
Weight	6.6 kg

* Available on the Bio-Plex Pro II wash station only.

Note: Additional features include plate-shaking capability and PC-based software for custom protocol development.

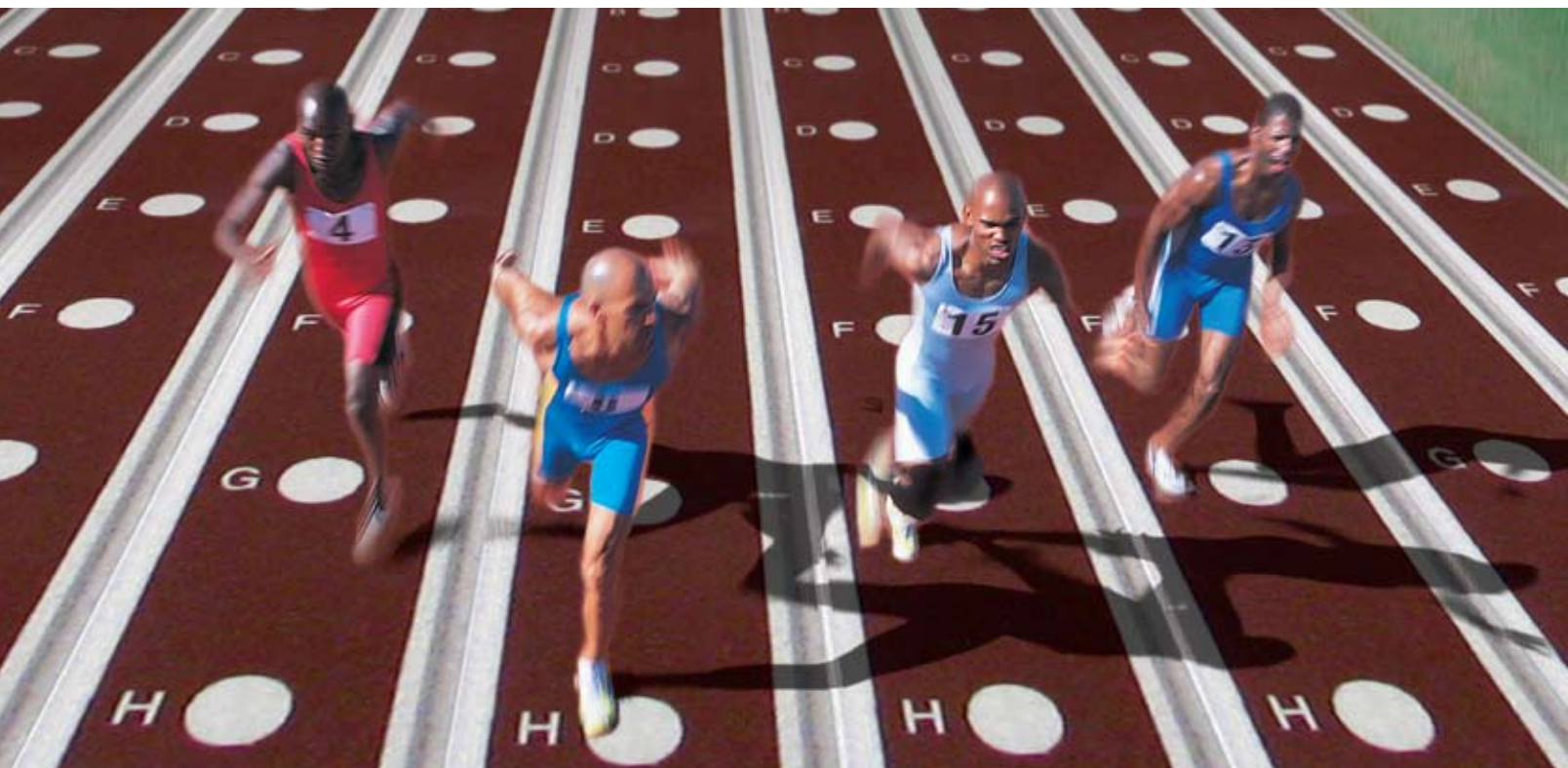
Bio-Plex Pro Wash Station Selection Guide

	Bio-Plex Pro Wash Station	Bio-Plex Pro II Wash Station
Bio-Plex assays (polystyrene beads)	—	•
MicroPlex microspheres	—	•
Bio-Plex Pro assays (magnetic beads)	•	•
Bio-Plex Precision Pro assays (magnetic beads)	•	•
MagPlex microspheres (magnetic beads)	•	•

Ordering Information

Catalog#	Description
300-34376	Bio-Plex Pro Wash Station, includes magnetic plate carrier, waste bottle, 2 buffer bottles
300-34377	Bio-Plex Pro II Wash Station, includes magnetic plate carrier, vacuum manifold plate carrier, waste bottle, 2 buffer bottles
171-025001*	Bio-Plex Pro Flat-Bottom Plates, 40 x 96-well plates

* Required for washing Bio-Plex Pro assays or other magnetic beads based assays using the magnetic plate carrier.



High Throughput From Start to Finish

In Biomarker Discovery, researchers are asked to do more with less, at record speeds. Traditional profiling techniques involve complex sample preparation protocols and long acquisition times that lengthen experimental timelines.

Bio-Rad's ProteinChip® SELDI system is designed with high-throughput protein biomarker discovery in mind.




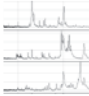
Take your marks — on-chip sample binding and washing eliminates the need for tedious chromatography-based cleanup steps.

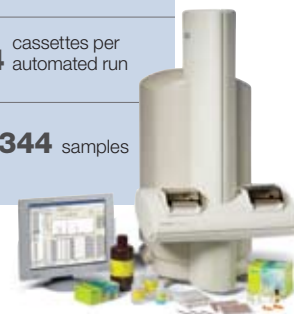
Ready — 96-well format is compatible with automated liquid handling robotics for high-throughput sample preparation.

Get set — data management software with integrated statistical tools means faster analysis of thousands of sample spectra.

Go! — fully automated data collection allows 1,344 samples to be run unattended in a matter of hours.

Accelerate your research. Visit us on the Web at www.bio-rad.com/proteinchip/

Discover high throughput	
	8 samples per chip
	x 12 chips per cassette
	x 14 cassettes per automated run
	= 1,344 samples



ProteinChip SELDI system, Enterprise Edition

The SELDI process is covered by U.S. patents 5,719,060, 6,225,047, 6,579,719, and 6,818,411 and other issued patents and pending applications in the U.S. and other jurisdictions.

ProteinChip® SELDI Kit Releases

The ProteinChip SELDI system product line now includes two new kits — one that offers an improved training tool and the other, a convenient way to perform mass calibrations.

ProteinChip System Starter Kit

The new ProteinChip system starter kit has been redesigned to deliver a focused step-by-step introduction to ProteinChip SELDI technology. The kit is a powerful training tool that incorporates video tutorials with reagents and instructions to generate protein profiles, then evaluate the results.

Video tutorials illustrate the basics of the ProteinChip SELDI system such as reading ProteinChip arrays, labeling peaks, and performing mass calibrations. Practice reading and collecting data from the included peptide standard array, then prepare your own ProteinChip NP20 and CM10 array from the included buffers, matrix, and samples (serum and *E. coli*). Use the analysis tools to determine the reproducibility and optimal peak count of your protein profiles, and compare your result to those obtained from the included premade ProteinChip arrays. Improve results with valuable tips and techniques outlined in the manual.



ProteinChip Peptide Mass Calibration Kit

The ProteinChip peptide mass calibration kit contains an array that provides external mass calibrations in the peptide region. The array contains seven peptides ranging from 1,084 to 12,230 Da. The array is ready-to-use directly from the package, with peptides and matrix included. A typical calibration takes as little as 10 minutes.

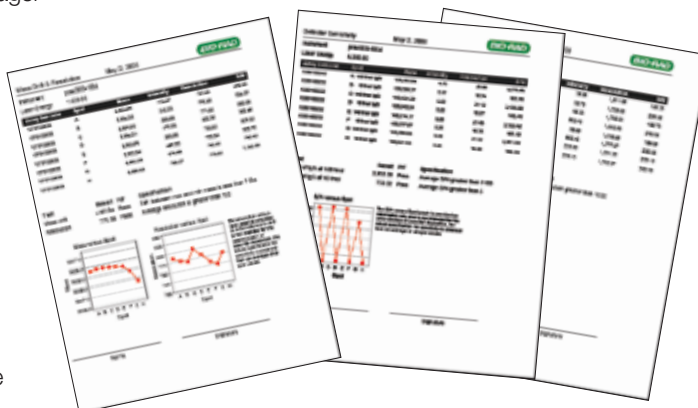


Ordering Information

Catalog #	Description
C70-00068	ProteinChip System Starter Kit
C70-00070	ProteinChip Peptide Mass Calibration Kit

ProteinChip® Data Manager Software, Version 3.5

The latest release of ProteinChip data manager software, version 3.5, offers automated reporting and one-click high-voltage conditioning. Use with the ProteinChip OQ and system check kits to run arrays and print results directly from the software. Print and file the reports for operational compliance, or paste them in your lab notebook to show instrument status during data collection. The program allows you to rename your spectra using the existing sample properties and to save spectrum processing parameters.



Ordering Information

Catalog #	Description
SW3-040010	ProteinChip Data Manager Software, Personal Edition
SW3-040030	ProteinChip Data Manager Software, Enterprise Edition

Extended Longevity of Gene Silencing Using Validated siLentMer™ siRNAs

Introduction

Silencing genes through the use of RNA interference-inducing molecules has become a standard practice within the biology research community. Gene silencing can be accomplished by a number of research methodologies; one of the most popular techniques (Elbashir et al. 2001) involves introducing synthetic small interfering RNAs (siRNAs) into the cells via a variety of methods, such as lipid-mediated transfection or electroporation. Upon entering the cell, these siRNAs silence the expression of a single gene by triggering the cellular RNA interference (RNAi) pathway. An mRNA sequence is targeted for degradation, thereby inhibiting gene expression (Elbashir et al. 2001, Filipowicz et al. 2005, Williams 2005). In time, the siRNA molecule is diluted by cellular division and degraded by endogenous endonucleases, thus decreasing its knockdown effect. As a rule, siRNAs that induce high levels of silencing at 1 or 2 days after transfection rarely maintain high silencing levels past day 4. This limits the breadth of experimentation that can be carried out using transient delivery. Unsustained silencing is particularly limiting when studying proteins that are slowly degraded. Also, the ability to achieve longer gene silencing is important for research studies that may lead to potential drug therapies.

Considering the advantages of sustaining expression beyond 4 days, the stable transfection method produces longer effects. The challenge with this method is establishing a successful stable transfection system, which can be very difficult and time consuming. Consequently, transient transfections are often preferred by researchers.

An ideal option would be the ability to attain longer effects using the simpler transient transfection method. One of the ways to achieve this is to use a more potent siRNA molecule that can produce longer posttransfection knockdown effects. The data presented in this article illustrate improved longevity of silencing using siLentMer validated Dicer-substrate siRNAs.

In RNAi studies, the key advantage to longer gene silencing from a transient transfection is sustained downregulation of a particular gene for longer periods of time. This extended duration helps to reduce the need to perform repeated transfections, which could lead to increased cellular toxicity. Also, evaluating knockdown effects for a longer period of time may permit researchers to study a larger variety of gene targets and perform expression comparisons that can't be accomplished within shorter time periods.

Comparison Study: Longevity of Gene Silencing

We compared the longevity of gene silencing achieved by two types of synthetic siRNA molecules: siLentMer validated Dicer substrates and traditional siRNAs. We studied the performance of the two types of siRNA in silencing five different genes over a 6 day period. siLentMer validated Dicer-substrate siRNAs, a uniquely designed siRNA molecule, were one type. Each of these siRNAs is 27 nucleotides long (27-mer) and serves as substrate for the Dicer enzyme. Dicer binds and cleaves each 27-mer into a 21-mer product (Figure 1), which is then incorporated into the RNA-induced silencing complex (RISC), and the functional guide strand targets the mRNA sequence for degradation (Agrawal et al. 2003, Fire et al. 1998, Hannon 2002, Napoli et al. 1990). The other type of molecule was a traditional siRNA, which is 19–22 base pairs long and does not serve as a Dicer substrate, although functionally it mimics the product of Dicer cleavage (Kim et al. 2005).

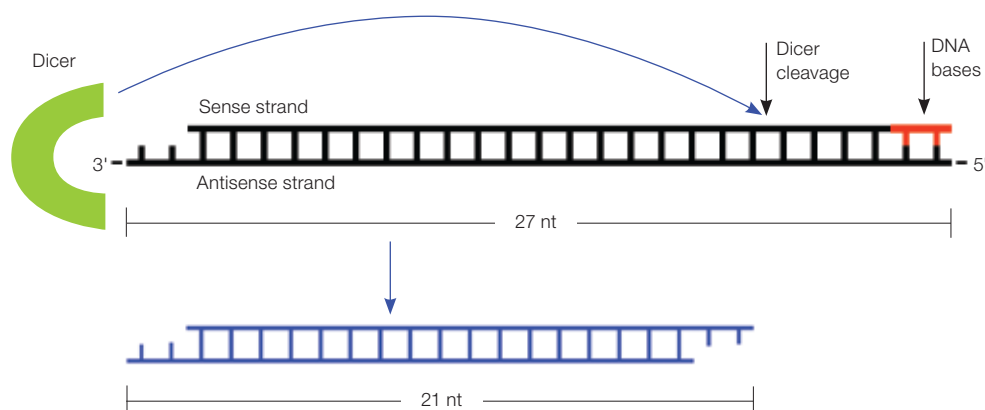


Fig. 1. Enzymatic cleavage of siLentMer Dicer-substrate siRNA. Dicer ribonuclease (■) is blocked by the two DNA bases on the 3' end (■) and binds to the opposite 3' overhang end (■). It then cleaves the molecule in a unidirectional manner to produce a single 21-nucleotide siRNA molecule (■).

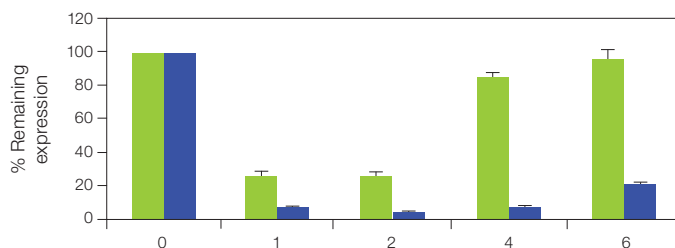
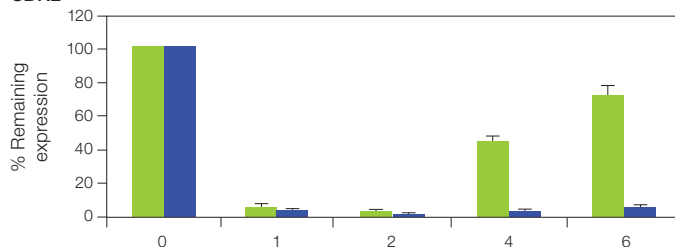
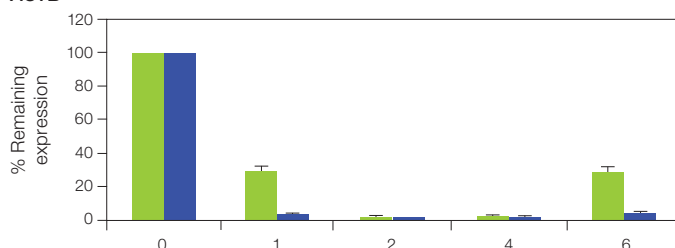
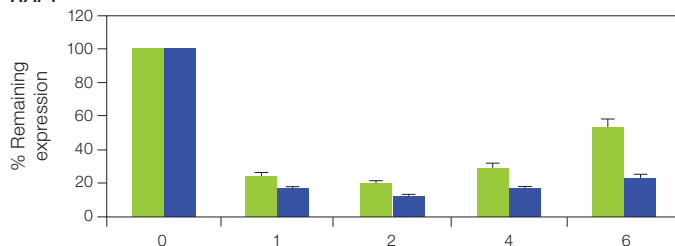
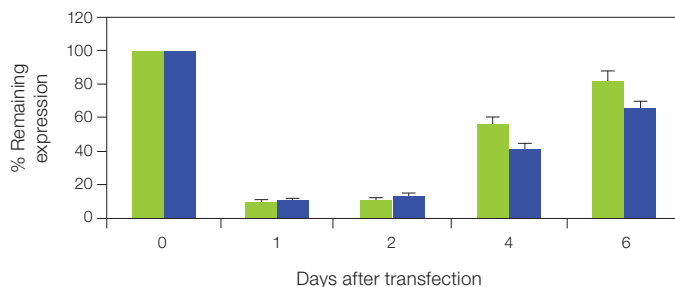
TP53**CDK2****ACTB****RAF1****AKT1**

Fig. 2. Silencing comparison study results. Extended silencing by Dicer-substrate 27-mers for the *TP53*, *CDK2*, *ACTB*, and *RAF1* gene targets; similar longevity of silencing by 21-mers (■) and Dicer-substrate 27-mers (■) for the *AKT1* gene targets for up to 6 days.

The ability of these siRNA molecules to sustain silencing was studied in HeLa cells by assessing reduction in mRNA expression levels via RT-qPCR for up to 6 days after delivering 5 nM of each target gene siRNA using siLentFect™ lipid reagent. There were significant differences in duration of silencing between the 27-mer and 21-mer for four of the genes (*ACTB*, *CDK2*, *TP53*, and *RAF1*); especially notable was the 27-mer knockdown performance at days 4 and 6 for each of these genes (Figure 2). For example, with the *TP53* gene, the 27-mer sustained an approximate 80% reduction in mRNA expression even at day 6, while the 21-mer only achieved just over 70% knockdown in the first 2 days. Similar performances were seen for the *AKT1* siRNAs, although the 27-mer showed slightly greater knockdown during the later days. Overall, the 27-mers outperformed the 21-mers for most gene targets by prolonging the knockdown effect. Previously published data on similar Dicer-substrate 27-mer siRNAs demonstrated extended knockdown for up to 9–10 days (Kim et al. 2005). Additionally, the 27-mers have been shown to achieve greater knockdown (over 85%) with lower siRNA concentrations (Kim et al. 2005, Kulisch et al. 2006, Rose et al. 2005).

Conclusion

Dicer-substrate siRNAs demonstrate very high potency using low concentrations as compared to 21-mers for many gene targets. As shown, these 27-mer Dicer-substrate siRNAs demonstrate substantially longer silencing for four of the five target genes tested when compared with 21-mers of the same sequence, offering the advantage of longer silencing at a lower dosage.

The siLentMer Dicer-substrate siRNAs are also validated through a rigorous process that includes quantitating gene silencing in HeLa cells to verify silencing that is greater than or equal to 85% using only 5 nM of siRNA per experiment. During this validation process, several potential dsRNA sequences are tested for performance to ensure a more predictable silencing result in subsequent experiments. This validated performance offers predictability, which helps eliminate the need to search for sequences that effectively silence specific genes.

References

- Agrawal N et al. (2003). RNA interference: biology, mechanism, and applications. *Microbiol Mol Biol Rev* 67, 657-685.
- Elbashir SM et al. (2001). Duplexes of 21-nucleotide RNAs mediate RNA interference in cultured mammalian cells. *Nature* 411, 494-498.
- Filipowicz W et al. (2005). Post-transcriptional gene silencing by siRNAs and miRNAs. *Current Opin Struct Biol* 15, 331-341.
- Fire A et al. (1998). Potent and specific genetic interference by double-stranded RNA in *Caenorhabditis elegans*. *Nature* 391, 806-811.
- Hannon GJ (2002). RNA interference. *Nature* 418, 244-251.
- Kim DH et al. (2005). Synthetic dsRNA Dicer substrates enhance RNAi potency and efficacy. *Nat Biotechnol* 23, 222-226.
- Kulisch S et al. (2006). Dicer-substrate siRNA technology. *BioRadiations* 120, 16-21.
- Napoli C et al. (1990). Introduction of a chimeric chalcone synthase gene into petunia results in reversible co-suppression of homologous genes in trans. *Plant Cell* 2, 279-289.
- Rose SD et al. (2005). Functional polarity is introduced by Dicer processing of short substrate RNAs. *Nucleic Acids Res* 33, 4140-4156.
- Williams BR (2005). Dicing with siRNA. *Nat Biotechnol* 23, 181-182.

ProteOn Manager™ Software — A Comprehensive Tool for the Analysis of Biomolecular Interactions

Introduction

ProteOn Manager software guides the user through complex protein interaction studies, allowing sophisticated experiments to be completed with ease. The software interface is comprehensive and includes control of instrument setup, experiment design, and data collection and analysis. As a result, the user is only required to learn one software package to generate and analyze data. The ProteOn Manager interface also provides a balance between automated and user-defined parameters. For example, users have a choice between predefined injection, flow rate, and temperature parameters or user-defined parameters — a selection of custom or pre-set protocol templates are available and processing and analyzing data can be done with a single button click or in a step-by-step manual fashion. No matter which approach a user may prefer (automated, manual, or combination of both), from beginning to end, ProteOn Manager software enables success with complex biomolecular interaction studies.

Instrument Control

The instrument control panel includes maintenance wizards that direct the user to weekly and monthly cleaning protocols to keep the instrument running at optimum performance. Additionally, the instrument control panel logs all instrument functions in a searchable and exportable database.

Protocol Design

The protocol editor (Figure 1) in ProteOn Manager software offers a variety of formats for easily creating a protocol. Users may design templates or custom protocols depending on their workflow. Also, samples may be imported or manually entered using copy and paste commands or group functions for iterative tasks. Pull-down menus help navigate samples into flexible locations.

Once samples are entered, data types and concentration can be selected to aid in downstream analysis. Orientation of flow graphics are shown to help visualize the sample location.

Sample Loading

Sample loading can be tedious and complex — especially if a user wants to conserve sample or reagents by performing multiple injections from a single location. To assist with the correct placement of samples, sample layout is visually displayed in several ways. First, position is indicated by color-coordinated graphics that represent the sample position in the protocol. Additionally, pull-down menus in the sample panels allow the user to easily switch sample locations while retaining all sample information (Figure 2).

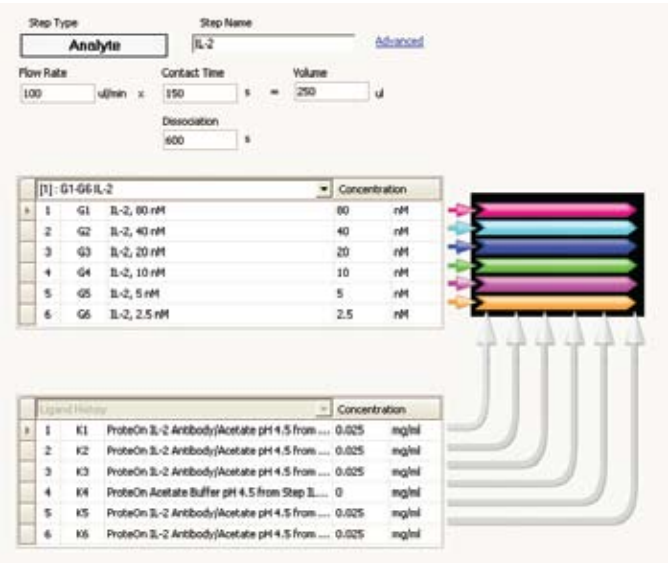


Fig. 1. Protocol editor showing navigation fields for sample entering and flow graphics.

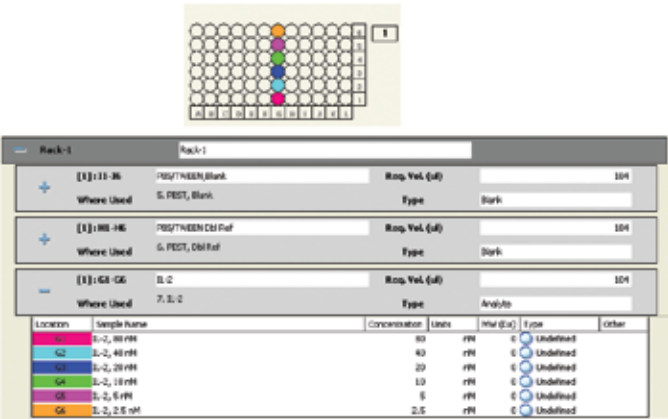


Fig. 2. Sample details are shown in a table format (bottom) and cross referenced by color and plate coordinates (top) to ensure the proper placement of samples or reagents.

Data Collection

With the help of the intuitive software interface, users can visualize real-time interactions of proteins on all 36 spots. Raw data collected from the instrument can be processed and analyzed with ProteOn Manager software. Data at any stage — raw, processed, or analyzed — can be exported.

Auto Processing

Sample processing in ProteOn Manager software is easy with single button capability and undo functions to illustrate the effects of different processing parameters to a data set (Figure 3). Users can instantly adjust the baseline and injection alignment parameters and remove artifacts using the autoprocess button.

For flexibility and procedural requirements, these functions can also be performed manually using a range value selected from the data set. All functions, including those manually executed, may be applied globally.

Referencing in the ProteOn Manager software is also adjusted with the click of a button. ProteOn Manager software supports a comprehensive set of referencing options, including interspot, channel referencing, real-time injection reference, double referencing and excluded volume correction for solvents like DMSO.

As flexibility in data processing is crucial for many laboratories, data may be exported either raw or processed for use outside of ProteOn Manager software. Sensorgrams in ProteOn Manager software may be exported in either a metafile or data format for use in presentations and publications.

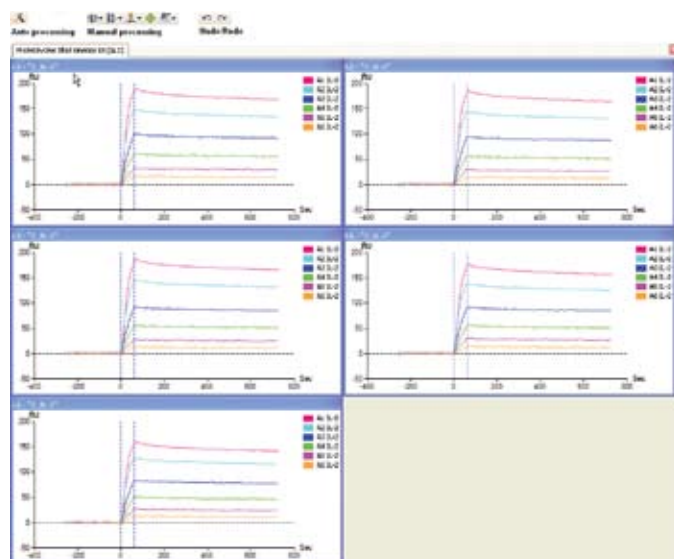


Fig. 3. Quick navigation to auto and manual processing controls through toolbar icons.

Analysis

Analysis of protein interactions is made simple through the use of intuitive software wizard interfaces (Figure 4). Wizards allow step-by-step data collection for kinetic, equilibrium, and concentration analysis. Biologically important parameters such as association and dissociation constants and affinity binding are reported in the data table, which can be easily exported. Each analysis mode allows the user to define analysis parameters, perform calculations, and review and print results. In addition to the analysis wizards report, analysis with molecular weight normalization is available. Seven different kinetic-fit models are supported, including Langmuir 1:1 and Langmuir with drift.

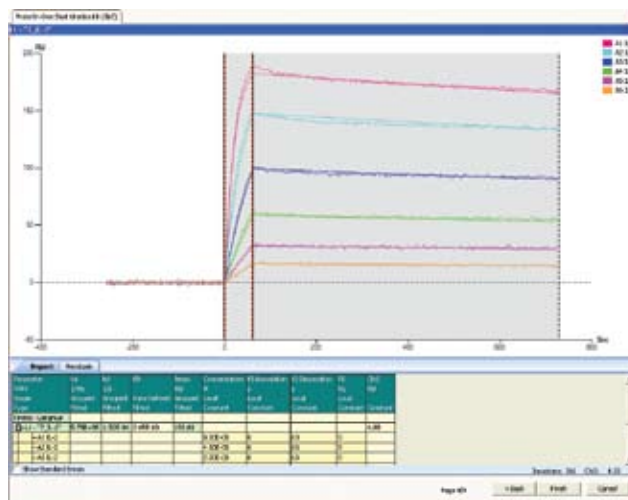


Fig. 4. Analysis wizards can be run on different processed data sets.

Regulatory Tools

Tools are available with the ProteOn Manager software to facilitate regulatory compliance in the drug discovery and development workflows. ProteOn Manager software, Security Edition and the ProteOn XPR36 installation qualification/operation qualification (IQ/OQ) kit (Figure 5) assist the user in adhering to the good practices rulings observed by the pharmaceutical industry. These rulings require procedural (notification, training, and operational), administrative, and technical (software-related) control changes.



Fig. 5. ProteOn Manager software, Security Edition and ProteOn XPR36 Installation Qualification/Operation Qualification (IQ/OQ) kit.

ProteOn Manager Software, Security Edition

New compliance features enable the user to turn on security features that comply with U.S. FDA 21 CFR part 11 regulations. Features of the Security Edition software include audit trails, electronic signatures, data validation, user log-ins and permissions, and closed-system security. Signatures can be verified, ensuring data consistency within the instrument.

ProteOn XPR36 Installation Qualification/Operational Qualification Kit

The ProteOn XPR36 IQ/OQ kit is designed to test critical system functions and to ensure the reliability and consistency of system performance. Key features include: intuitive wizard-driven software, printable electronic reports for document control, electronic log of IQ/OQ and test results, ready-to-use reagents, and sensor chip for testing system performance with walk-away unattended operation.

Automated Affinity Purification of Native-Like Recombinant Proteins Using the Profinity eXact™ Fusion-Tag System With the Profinia™ Protein Purification System

The novel Profinity eXact fusion-tag system is used to generate affinity-purified proteins containing native amino acid sequences. Performing Profinity eXact system purifications on the Profinia protein purification system automates the process (Figure 1). The Profinia instrument provides preprogrammed methods for one-step purification — including cartridge equilibration, sample loading, washing, tag cleavage by enzyme, and elution — so no operator intervention is necessary. Users can select preprogrammed Bio-Rad methods or create customized program methods to purify proteins with recommended buffers (bulletin 5725). Bio-Scale™ Mini Profinity eXact cartridges are used with the Profinia system to purify tag-free proteins in as little as 1 hour. The resulting purity and yield are comparable to those achieved by other purification methods, but with less time and effort required.



Fig. 1. Profinity eXact fusion-tag system purification on the Profinia protein purification system.

To illustrate the purification of Profinity eXact system fusion proteins by the Profinia system, we paired the systems to purify a native-like (without artificial amino acids and with correct conformation) recombinant protein. Profinity eXact-MetC protein (*Shewanella oneidensis*) expressed in *E. coli* BL21(DE3)pLysS cells (Novagen) was purified using 1 ml Profinity eXact cartridges installed on the Profinia system. Column pre-equilibration, sample binding, washing, and elution steps were performed according to system protocols (bulletin 5725). MetC was eluted and desalted using the Profinity eXact cartridge plus the desalting method in the program methods (manual programming) mode of the Profinia system.

Figure 2 shows that the Profinity eXact-MetC protein can be purified within 40 minutes, which includes the enzyme cleavage of tag in as little as 12 minutes (Figure 2A). Similar yields were achieved when cleavage time was extended to 30 minutes or

2 hours (data not shown). Protein purity was evaluated using the Experion™ automated electrophoresis system. Results demonstrated more than 90% purity for all cleavage times (Figure 2B).

Various proteins have been purified using the Profinity eXact fusion-tag system on the Profinia system, and some have also been subsequently confirmed to have biological functions (bulletin 5742). Tag-free proteins generated by the automated purification process can be immediately used downstream after affinity purification and desalting, which is valuable for functional and structural studies where native sequences are preferred.

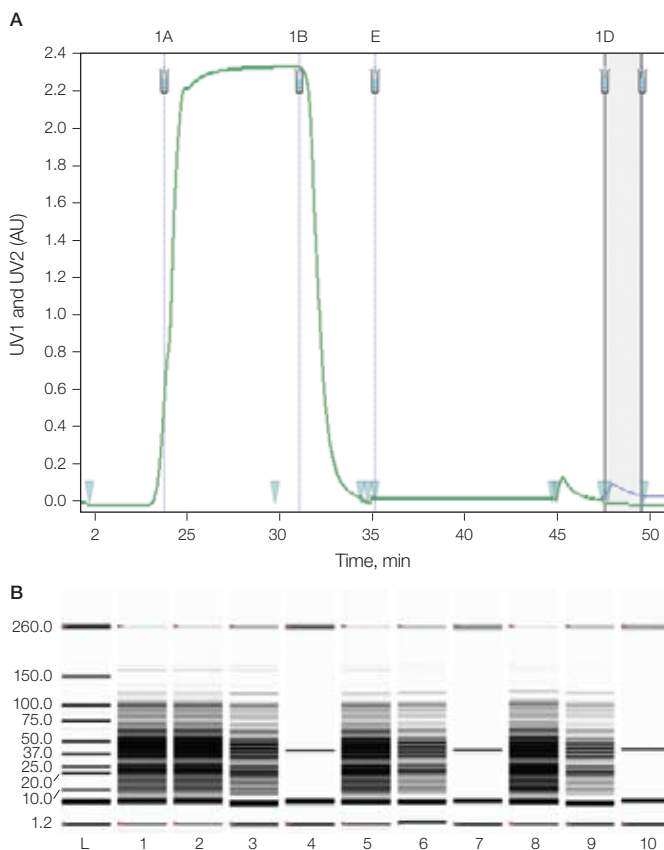


Fig. 2. Purification of MetC protein from *E. coli*. Profinity eXact-MetC from 30 ml of lysate was loaded on 1 ml Bio-Scale Mini Profinity eXact cartridges and tag cleavage was conducted for 12 min before MetC was eluted and desalted using the Profinity eXact system cartridge plus the desalting method in the program methods mode of the Profinia system. **A**, chromatogram; the fractions are 1A (flowthrough), 1B (wash), and 1D (elution). **B**, Experion gel image derived from electropherograms of collected fractions. Lane L, molecular weight standard; 1, load, 12 min; 2, flowthrough, 12 min; 3, wash, 12 min; 4, elution, 12 min, cleavage; 5, flowthrough, 30 min; 6, wash, 30 min; 7, elution, 30 min, cleavage; 8, flowthrough, 2 hr; 9, wash, 2 hr; 10, elution, 2 hr, cleavage.

Low-Volume Amplification of DNA Using the C1000™ Thermal Cycler

Daniel E Sullivan, Bio-Rad Laboratories, Inc., Hercules, CA 94547 USA

Introduction

PCR amplification is a powerful tool used in a variety of molecular biology techniques, such as cloning, gene expression profiling, site-directed mutagenesis, and genetic mapping. For most applications, PCR is performed in 20–50 µl reaction volumes, which provide ample product for post-PCR analysis and manipulation. However, for PCR-based screening applications, only enough DNA needs to be produced to adequately test for the presence of a DNA fragment after the reaction. In these applications, there are clear advantages to performing reactions in smaller volumes, as the miniaturization of PCR allows increased throughput and reduced reagent costs.

In many cases, low-volume PCR (1–5 µl) can yield variable results due to problems with thermal uniformity and accuracy of many thermal cyclers, as well as poor reaction vessel sealing.

The Bio-Rad 1000-series thermal cycling platform (comprising the full-featured C1000 and the basic S1000™ thermal cyclers) has been engineered for extremely uniform and reliable thermal performance. The 1000-series thermal cyclers have six independently controlled thermal electric units to maintain temperature uniformity at all times during the run, even during ramping. The average ramp rates, combined with a 10 sec settling time, deliver fast run times while also maintaining excellent thermal accuracy and uniformity. These instruments are ideally suited for successful PCR in low volumes.

We evaluated the ability of the C1000 thermal cycler equipped with a 384-well reaction module to successfully amplify four target sequences from human genomic DNA in 1, 2, 5, and 10 µl reaction volumes. We demonstrated robust and reproducible amplification of the four genomic DNA targets at all of the reaction volumes tested.

Methods

All PCR amplifications were performed on a C1000 thermal cycler equipped with a 384-well reaction module using 384-well Hard-Shell® thin-wall skirted PCR plates sealed with Microseal® 'B' adhesive seal. The melting temperature (T_m) of each primer (Table 1) was determined using the Ta Calc feature of the Protocol Autowriter available on the C1000 thermal cycler.

Reactions were prepared using iQ™ supermix which is supplied as a 2x ready-to-use solution with optimal concentrations of reaction components, 0.25 µM of each primer, and human genomic target concentrations of 1,000 or 2,000 human genome equivalents per µl (K562 DNA, Promega Corporation). Reaction components were assembled as a master mix, then dispensed in the desired volumes into the appropriate reaction plate wells. Three replicate reactions were performed for the 2, 5, and 10 µl volumes for each of the amplicons. Six replicate reactions were prepared for the 1 µl volume. Control reactions that contained all of the reaction components except the target DNA were performed for each volume. The 1 and 2 µl reaction volumes were manually pipetted using a P2 Pipetman (Gilson, Inc.). Calibration of the pipets was checked with Microcapillary Drummond pipets (Sigma-Aldrich Co.). The plate was sealed with Microseal 'B' adhesive seal and spun at 750 x g for 2 min prior to and after thermal cycling.

The protocol used for amplification included the following steps: 95°C for 3 min; (95°C for 10 sec, 55°C for 20 sec, 72°C for 30 sec) x 35; 72°C for 10 min; 4°C hold. The lid temperature was set to 100°C. The annealing temperature was 55°C (2.5°C below the average T_m of the primer pair with the lowest T_m , β-globin-261-60). The final 10 min incubation at 72°C was used to ensure significant amplicon reassociation. The reaction module adjustable lid was rotated approximately two-thirds turns past the touch point to provide appropriate sealing pressure for the Microseal 'B' adhesive seal.

Table 1. Target genes with primer and amplicon characteristics.

Target Gene	Amplicon Name	Amplicon Size, bp	Primer Sequence*	Primer T_m	Average T_m of Primer Pair
β-globin	β-globin-261-60	261	F: GAG GAG AAG TCT GCC GTT AC R: GAC AGA TCC CCA AAG GAC TC	56.5 58.5	57.5
Mannose receptor binding protein	TIP-171	171	F: TTT TCC AGC ATC CAC TCC TTC R: GGC TTT CTC AGT GAT TCC AGG	61.3 61.0	61.2
Glyceraldehyde phosphate dehydrogenase	GAPDH-494-60	494	F: CTG GAG CCT TCA GTT GCA G R: GAA GAT GGT GAT GGG ATT TC	59.7 56.9	58.3
Amelogenin	AMEL	106–112	F: CCC TGG GCT CTG TAA AGA ATA GTG R: ATC AGA GCT TAA ACT GGG AAG CTG	62.7 62.6	62.7

* F = forward, R = reverse.

A set of loading dye solutions was prepared at various concentrations. After thermal cycling, appropriate volumes of the loading dye solutions were added to the reactions such that 5 µl at 1x loading dye concentration (containing 0.1% Orange G and 3% glycerol in 1x PCR buffer) could be loaded onto the gel (Table 2). Orange G was used as a gel loading dye because it migrates in these gels well ahead of the 50 bp size marker. The traditional loading solution dye, xylene cyanole, migrates with 200–300 bp of DNA and can lessen the apparent intensity of the ethidium bromide fluorescence of comigrating DNAs.

Table 2. Preparation of samples for loading onto gel.

Reaction Volume, µl	Loading Dye*			Volume Loaded Onto Gel, µl
	Stock Concentration	Volume Added, µl	Final Concentration	
10	5x	2.5	1x	5
5	5x	1.25	1x	5
2	1.4x	5	1x	5
1	1.2x	6	1x	5

* 1x loading dye solution = 0.1% Orange G, 3% glycerol, 50 mM KCl, 10 mM Tris-HCl, pH 8.0.

Analysis of amplified DNA fragments was performed using 3% ReadyAgarose™ 96 Plus precast gels in TBE buffer containing ethidium bromide (0.5 µg/ml). For each reaction, 5 µl of PCR product loading dye mix was loaded onto the gel, and electrophoresis was performed at 60 V for 40 min. An AmpliSize® molecular ruler 50–2,000 bp ladder was used to determine amplicon sizes. Gels were imaged using the Molecular Imager® Gel Doc™ XR system.

The yield of each amplification reaction was measured by fluorogenic intercalation of Hoechst 33258 dye (Sigma-Aldrich Co.) using the DyNA Quant 200 fluorometer (Hoefer, Inc.).

Results and Discussion

All of the reactions performed using 1, 2, 5, and 10 µl reaction volumes amplified a DNA fragment of the expected size (Table 1) in sufficient quantities to be visible on a gel (Figure 1).

Although all of the reactions produced sufficient specific products to see on the ethidium bromide-stained gel, we wanted to obtain a more quantitative understanding of the relationship between reaction volume and PCR yield. To this end, additional

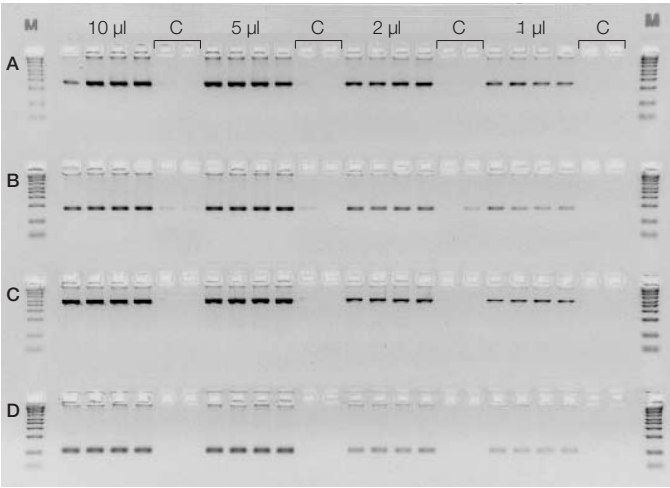


Fig. 1. Ethidium bromide fluorescence gel image of the reaction products. After adding dye-loading solution to 1x (see Table 2), 5 µl of the resulting mix was run on a 3% agarose TBE gel and imaged with the Molecular Imager Gel Doc XR system (3.5 sec exposure). **A**, β-globin, 261 bp; **B**, TIP-171, 171 bp; **C**, GAPDH, 494 bp; **D**, AMEL, 106–112 bp. Lanes marked C are control reactions (no target). All other reactions began with ~1,000 human genomes/µl. M, molecular ruler.

reaction volume sets were run and the concentration of dsDNA products was determined for each reaction volume. We analyzed three replicates of the 2, 5, and 10 µl reactions, and six replicates of the 1 µl reactions for each. The yields of amplified double-stranded PCR product ranged between 6 and 23 ng/µl (Table 3 and Figure 2). These values are consistent with the gel image (Figure 1) and with the detection limits of dsDNA on this agarose/ethidium bromide gel, which are in the range of 1–5 ng per band.

For at least three of the four amplicons there appears to be a trend toward slightly lower yields as the reaction volume decreases. This phenomenon could be due to reduction in reaction efficiency due to slight evaporative losses. The data indicate that in the 1 and 2 µl reaction volumes, the yield reduction varies for each amplicon and ranges from about 15 to 30% compared to the 10 µl reactions. However, for all amplicons tested, the yields in the 1 and 2 µl reactions are sufficient to produce the specific and easily visible bands in an agarose/ethidium bromide gel.

Table 3. Amplicon yields expressed in ng/µl.

Amplicon	10 µl Reactions*			5 µl Reactions*			2 µl Reactions*			1 µl Reactions**		
	Average	Range	SD	Average	Range	SD	Average	Range	SD	Average	Range	SD
β-globin-261-60	14.7	14–16	1.16	13.7	13–15	1.16	12	11–13	1	10.3	10–12	1.16
TIP-171	8.7	6–11	0.58	9.7	9–11	1.16	7.3	6–8	1.16	8	6–12	3.06
GAPDH-494-60	21.3	19–23	1.53	19.3	19–20	0.58	16	15–17	1	16.7	16–18	1.16
AMEL	15.5	14–17	1.53	14	13–15	1	12.3	12–13	0.58	10.5	8–14.7	3.40

* n = 3.

** n = 6.

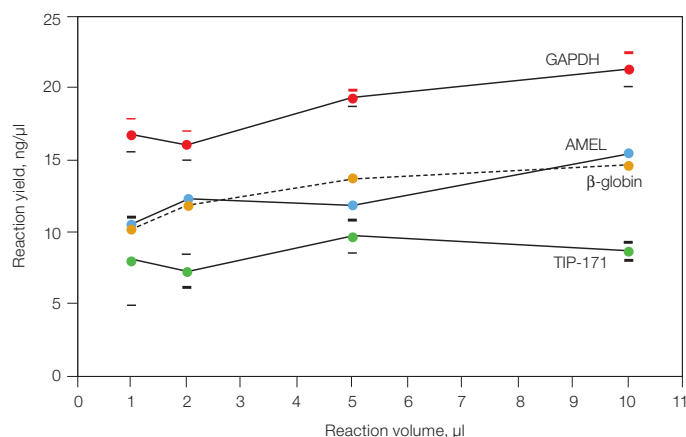


Fig. 2. Average concentrations of PCR products at four reaction volumes as determined by fluorogenic intercalation of Hoechst 33258 dye. For all volumes, three replicates were measured, except the 1 μl reactions, where six replicates were measured. The bars on the GAPDH and the TIP-171 data are ± 1 standard deviation. They are not shown for the amelogenin and the β -globin data for clarity, but are of the same magnitude as those shown.

Evaporation is a major concern when performing PCR amplifications in low volumes. Even when a tight seal is created using an adhesive sealer, small reaction volumes may be significantly affected by residual evaporation that takes place until the saturation vapor pressure is reached in the reaction vessel. The small volume of the wells in the 384-well plate minimizes evaporative loss from the reaction. The use of Microseal 'B' sealer combined with proper pressure from the reaction module lid results in no visible loss of reaction volume at the end of the thermal cycling protocol. If higher sensitivity in gel analysis is required to detect smaller fragments or amplicons that do not amplify as efficiently, more sensitive fluorescent dyes, such as PicoGreen (Ahn et al. 1996) or SYBR® Green I can be used to stain the gels.

Ways to potentially increase reaction yields at all volumes include starting with higher initial target concentrations, increasing primer concentrations, and increasing the number of repeat cycles in the protocol, especially if the initial target concentration is low (for example, <100 targets/ μl).

Conclusions

We demonstrated that the C1000 thermal cycler equipped with a 384-well reaction module can accurately and reproducibly amplify target sequences from genomic DNA in as little as 1 μl reaction volumes. We showed that even fragments in the 100 bp size range can be amplified in quantities sufficient to be easily detectable on an agarose/ethidium bromide gel.

Reducing the total reaction volume used for a PCR assay can greatly reduce reagent costs in high-throughput experiments. Success in miniaturization of reaction volumes depends on precise thermal control of the thermal cycler, stability of the reagents at small scales, superior sealing of reaction vessels to prevent evaporation, and the ability of the reaction to withstand residual evaporation.

The precise temperature control of the 1000-series thermal cyclers allows fast temperature ramping while maintaining tight uniformity across the heating block throughout the ramp. This results in reaching the target temperature and beginning the incubation time more quickly, for faster overall run times. The C1000 and the S1000 reaction modules have fully adjustable heated lids that snap tight when locking. The lid is designed to lock below a housing lip that provides strong and even downward force on the block, thereby minimizing evaporative sample loss and supporting low-volume PCR amplifications.

Reference

Ahn SJ et al. (1996). PicoGreen quantitation of DNA: effective evaluation of samples pre- or post-PCR. *Nucleic Acids Res* 24, 2623-2625.

Molecular Weight Estimation Using Precision Plus Protein™ WesternC™ Standards on Criterion™ Tris-HCl and Criterion™ XT Bis-Tris Gels

Lily Lai, Nik Chmiel, Michael Urban, Tim Wehr, John Walker, and Jeff Xu, Bio-Rad Laboratories, Inc., Hercules, CA 94547 USA

Introduction

One-dimensional gel electrophoresis is frequently used to obtain information about the molecular weight and purity of proteins (Hames and Rickwood 1990). In PAGE, proteins migrate in response to an electric field, and the composition of the gel matrix acts as a sieve to separate proteins based on size, charge, and shape. The protein standards used in PAGE are fundamental tools of protein research and are critical in estimating the size of a protein of interest. Following electrophoresis on a gel, separated proteins are frequently blotted to a membrane and identified using antibodies and immunodetection reagents. Under these conditions, accurate and precise molecular weight estimation across a variety of different gel formulations depends upon the use of a high-quality protein standard.

Criterion and Criterion XT precast gels from Bio-Rad Laboratories provide convenient, high-resolution and high-throughput protein separation. The gels are available in a variety of single-percentage and gradient acrylamide concentrations, buffer compositions, and well configurations. In addition, Criterion XT precast gels utilize a neutral pH gel formulation to offer the same separation capabilities as other Criterion gels, but with an extended shelf life and room-temperature storage.

Precision Plus Protein WesternC standards have ten prestained Strep-tagged protein bands that can be used to monitor migration during electrophoresis, and provide a simple method for assessing transfer efficiency after blotting. With the addition of StrepTactin horseradish peroxidase (HRP) during the secondary antibody incubation step, all ten bands of the standard can be detected by chemiluminescence. This capability provides an easy method for estimating the molecular weight of a protein of interest on gels and western blots (Urban and Woo 2007).

In this study, the migration patterns of the Precision Plus Protein WesternC standards on selected Criterion and Criterion XT gel types were compared. The relative migrations of protein bands in the standards were used to estimate the molecular weight of bovine serum albumin (BSA) on western blots generated from each gel type. The results demonstrate that the Precision Plus Protein WesternC standards can be used on a variety of Criterion and Criterion XT gel types and provide a convenient method to estimate the molecular weight of proteins directly from blots.

Methods

A total of 200 ng of BSA (Bio-Rad Laboratories, Inc.), and 5 µl of WesternC standards were loaded onto Criterion Tris-HCl 4–20% linear gradient, Criterion XT Bis-Tris 10%, and 4–12% resolving gels. Electrophoresis was performed using a Criterion cell at

200 V on the PAGE systems in Table 1 until the dye front reached the bottom of the gel (35–60 min depending on gel type).

For chemiluminescence detection of both Precision Plus Protein WesternC standards and BSA samples, the gels were blotted using a Criterion blotter onto 0.45 µm nitrocellulose membranes at 100 V for 30 min using Towbin buffer (25 mM Tris-HCl [pH 8.3], 192 mM glycine, 20% [v/v] methanol). The blots were blocked in 1% (w/v) casein in TBS (20 mM Tris-HCl [pH 7.5], 500 mM NaCl) for 1 hr and washed 3 x 5 min in TTBS (20 mM Tris-HCl [pH 7.5], 500 mM NaCl, 0.05% [v/v] Tween) before addition of a 1:200 dilution of primary BSA antibody (Sigma-Aldrich Co.) in TTBS. After incubation for 1 hr, the blots were washed 6 x 5 min prior to addition of a 1:50,000 dilution of HRP-conjugated goat anti-rabbit antibody in TTBS (Bio-Rad) and a 1:10,000 dilution of the Precision Plus Protein StrepTactin-HRP conjugate in TTBS, followed by 1 hr incubation. Blots were washed in TTBS 6 x 5 min before addition of Immun-Star™ WesternC™ chemiluminescent detection solutions, and were immediately imaged on a Molecular Imager® ChemiDoc™ XRS system. Relative migration calculations of both standards and BSA were performed using Quantity One® 1-D analysis software and plotted in Microsoft Excel (bulletin 3133). The actual molecular weight of BSA was determined by mass spectrometry using an Autoflex MALDI-TOF system (Bruker Daltonik GmbH).

Table 1. Criterion and Criterion XT gels and buffers tested.

Gel	Buffer	Buffer Abbreviation
Criterion 4–20% Tris-HCl	Tris/Glycine/SDS	TGS
Criterion XT 4–12% Bis-Tris	2-(N-morpholino)ethanesulfonic acid	MES
Criterion XT 10% Bis-Tris	2-(N-morpholino)ethanesulfonic acid	MES
Criterion XT 4–12% Bis-Tris	3-(N-morpholino)propanesulfonic acid	MOPS

Results and Discussion

Figure 1 shows the migration patterns of the Precision Plus Protein WesternC standards and BSA on each of the four PAGE systems following transfer and chemiluminescence detection on western blots. The relative front (R_f) values for the Precision Plus Protein WesternC standards and BSA determined for each gel type are shown in Tables 2 and 3. By plotting the R_f versus the log molecular weight (MW) values, a standard curve for the Precision Plus Protein WesternC standards was generated to estimate the MW of BSA. Linear fits to the Precision Plus Protein WesternC standards data points on blots were obtained from each gel type, and R^2 values were calculated to assess the accuracy of the fits. The molecular weight of each BSA sample was determined from the linear fits obtained from the standards.

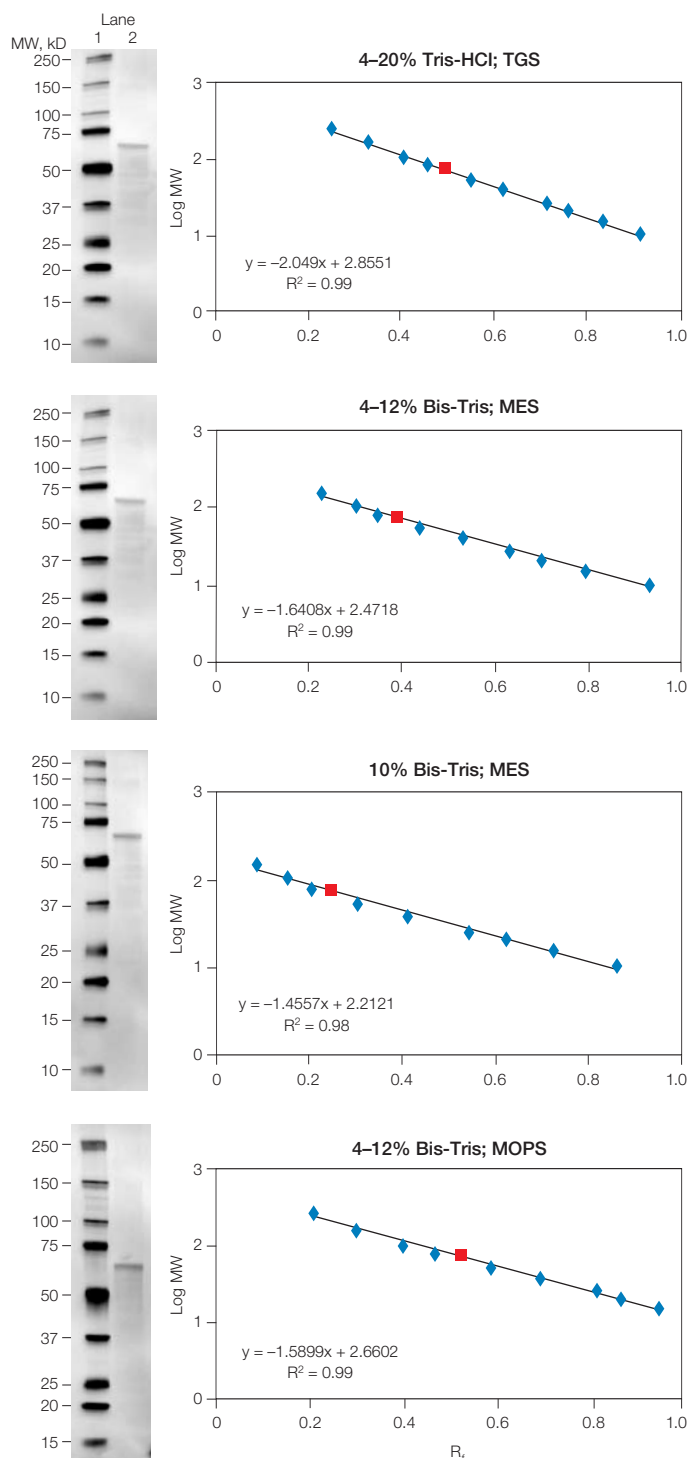


Fig. 1 Determining the MW of BSA using Precision Plus Protein WesternC standards on western blots obtained from different Criterion gel types. Standard curves of log MW versus relative front (R_f) were generated using Precision Plus Protein WesternC standards from chemiluminescence-detected western blots. Linear fits to the standards data points (♦) were used to estimate the MW of BSA (■) on each Criterion gel type tested from the equations calculated from the standard curves. The corresponding gel migration patterns of the standards (lane 1) and BSA (lane 2) are shown on chemiluminescent detected blots to the left of each standard curve plot for the four gel types. The high R^2 values (>0.98) obtained from the standard curves demonstrate the exceptional linearity of the Precision Plus Protein WesternC standards.

Table 2. Measurement of R_f values for the Precision Plus Protein WesternC standards from western blots. Each blot was independently analyzed.

MW of Standards		R_f Value			
MW	Log MW	4-20% Tris-HCl	4-12% MES	10% MES	4-12% MOPS
250	2.398	0.256	omitted	omitted	0.209
150	2.176	0.329	0.226	0.091	0.302
100	2.000	0.407	0.304	0.157	0.399
75	1.875	0.460	0.350	0.206	0.461
50	1.699	0.548	0.437	0.305	0.582
37	1.568	0.621	0.531	0.415	0.688
25	1.398	0.712	0.631	0.543	0.805
20	1.301	0.759	0.697	0.624	0.858
15	1.176	0.833	0.798	0.725	0.948
10	1.000	0.912	0.934	0.860	unresolved

Table 3. Measurement of R_f and comparison of actual versus calculated MW of BSA from western blots using Precision Plus Protein WesternC standards.

	BSA, ng	R_f	Calculated MW WesternC Standards	Actual MW Mass Spectrometry	Difference
4-20% Tris-HCl	200	0.494	69.65	66.43	5%
4-12% Bis-Tris MES	200	0.388	68.42	66.43	3%
10% Bis-Tris MES	200	0.253	69.79	66.43	5%
4-12% Bis-Tris MOPS	200	0.521	67.90	66.43	2%

While all ten bands of the Precision Plus Protein WesternC standards were resolved on most Criterion gel types, the best linear fit with Criterion XT 10% and 4-12% gels run in a MES buffer was obtained after omitting the band at 250 kD due to the decreased linearity of the electrophoretic separation on these gel types for large molecular weight bands. The 10 kD band was unresolved on Criterion XT 4-12% gels with a MOPS running buffer. MOPS provides greater separation of the large molecular weight bands at the expense of resolution of the low molecular weight bands. For all gel types tested, the R^2 values for the linear fit of the Precision Plus Protein WesternC standards were >0.98. Based on these fits, the molecular weight calculations of BSA were within 5% or less of the actual mass of the protein as determined by mass spectrometry (Table 3).

Conclusions

The results demonstrate that Precision Plus Protein WesternC standards provide an accurate method for estimating protein molecular weight on blots obtained from using either Criterion or Criterion XT gels.

References

- (2004). Molecular weight determination by SDS-PAGE. Bio-Rad Bulletin 3133.
- Hames BD and Rickwood D (1990). Gel electrophoresis of proteins, a practical approach, 2nd edition. Oxford University Press, 1-147.
- Urban M and Woo L (2007). Molecular weight estimation and quantitation of protein samples using Precision Plus Protein WesternC standards, the Immuno-Star WesternC chemiluminescent detection kit, and the Molecular Imager ChemiDoc XRS imaging system. Bio-Rad Bulletin 5576.

ProteoMiner™ Protein Enrichment Technology

GOES GLOBAL

Path to Discovery

Hailed as the completion of a major scientific milestone, the sequencing of the human genome has in many respects marked the beginning of a new, more complex era of research. With roughly 25,000 human genes identified and the sequencing of many other types of plant and animal genomes either completed or under way, this research frontier requires not only identification of the estimated tens of thousands of proteins coded by these genes, but also determination of how gene expression or suppression correlates with the manifestation or prevention of disease. Because of alternative splicing events and posttranslational modifications, the highly complex proteome is more dynamic than the genome, and is therefore an additional rich source of potential biomarkers for clinical use. It is hoped that proteomics research will lead to the discovery of sensitive protein biomarkers that will aid in the diagnosis and prognostic assessment of disease, as well as in the development of more effective therapeutic interventions.

The task of identifying proteins related to disease has proved difficult, because a relatively small number of high-abundance proteins in biological samples usually comprise a large percentage of total protein mass. For example, the proteins in human serum and plasma — the primary sample sources used in clinical proteomic studies — span a concentration range of 11 orders of magnitude. Furthermore, the 20 most abundant proteins represent 97–99% of the total protein mass (Anderson and Anderson 2002). When common analytical methods are used, these high-abundance proteins can inhibit detection of low-abundance proteins that may be related to physiological dysfunction.



ProteoMiner protein enrichment system technology was developed to decrease levels of high-abundance proteins during the preparation of biological samples for proteomic analysis (Figure 1). This technology has been shown not only to render low-abundance proteins detectable, but also to increase their concentration, unmasking and enabling the discovery of hundreds of proteins. Results from studies using ProteoMiner protein enrichment technology indicate that the number of existing proteins has been significantly underestimated (Sennels et al. 2007). The capacity of this sample preparation tool to help unveil the proteome has led to its worldwide use in laboratories that are involved in the discovery of protein biomarkers for diseases.

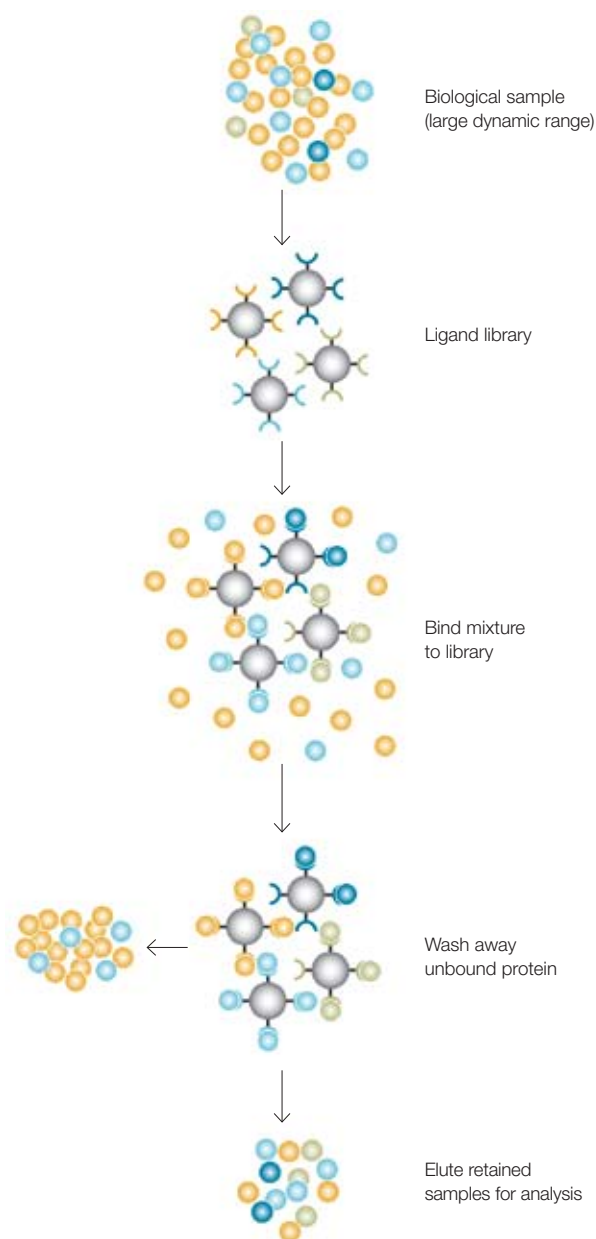


Fig. 1. ProteoMiner protein enrichment system technology. Each bead features a different hexapeptide ligand with affinity for specific proteins in a sample. When a complex protein sample is incubated with a bead library, protein components find their binding partners. Excess high-abundance proteins will not be captured on binding sites and will be depleted once the beads are washed. In contrast, low-abundance proteins will be concentrated on their specific affinity ligand. In this way, low-abundance proteins are enriched relative to the high-abundance proteins in the sample. No fraction is discarded in this approach, and proteins that might bind to high-abundance proteins like albumin are retained.

ProteoMiner Protein Enrichment Technology

By decreasing high-abundance proteins and capturing low-abundance proteins, this novel sample preparation tool compresses the dynamic range of protein concentrations in complex biological samples, leading to an enrichment of medium- and low-abundance proteins. The technology utilizes a library of hexapeptides that are created through combinatorial synthesis, and bound to a chromatographic support. The result is a very large library of hexapeptide ligands that act as unique binders for proteins. The bead population has such diversity that a binding partner should exist for most, if not all, proteins in a sample. Each bead has an equivalent binding capacity; that is, the capacity for binding high- and low-abundance proteins in the sample is equal. Since there are a limited number of binding sites per protein, high-abundance proteins quickly reach saturation, while low-abundance proteins continue to bind. Those high-abundance proteins that reach saturation cease binding, and the unbound excess protein molecules are washed out (Figure 1). After elution, the medium- and low-abundance proteins are enriched while the concentration of high-abundance proteins is reduced. This allows detection and identification of low-abundance proteins that cannot be discovered using other methods (Figure 2).

Prior to the release of ProteoMiner protein enrichment kits, immunodepletion was the most commonly employed method

for depleting high-abundance proteins. Immunodepletion utilizes immobilized antibodies to selectively remove a subset of high-abundance proteins. However, immunodepletion does nothing to enrich low-abundance proteins, and actually results in their dilution. Furthermore, the capacity of the immobilized antibodies is very low, which limits the amount of sample that can be added. Researchers must process their samples multiple times in the attempt to retrieve low-abundance proteins in detectable amounts. Another disadvantage to immunodepletion is that many proteins associated with high-abundance proteins are inadvertently removed during the depletion step.

In contrast to immunodepletion, large sample volumes can be processed by the ProteoMiner protein enrichment kit, thus increasing the opportunity for capture and subsequent detection of low-abundance proteins (Figure 2). This enrichment technology is applicable to different types of sample, and has been used successfully with serum, plasma, urine, CSF, bile, and other sample types. With regard to samples, immunodepletion is more restrictive because antibodies used for depletion must be designed for specific sample types and species. Another key advantage of the ProteoMiner kit is that samples are eluted in small volumes, therefore no additional concentration steps are required for most downstream applications.

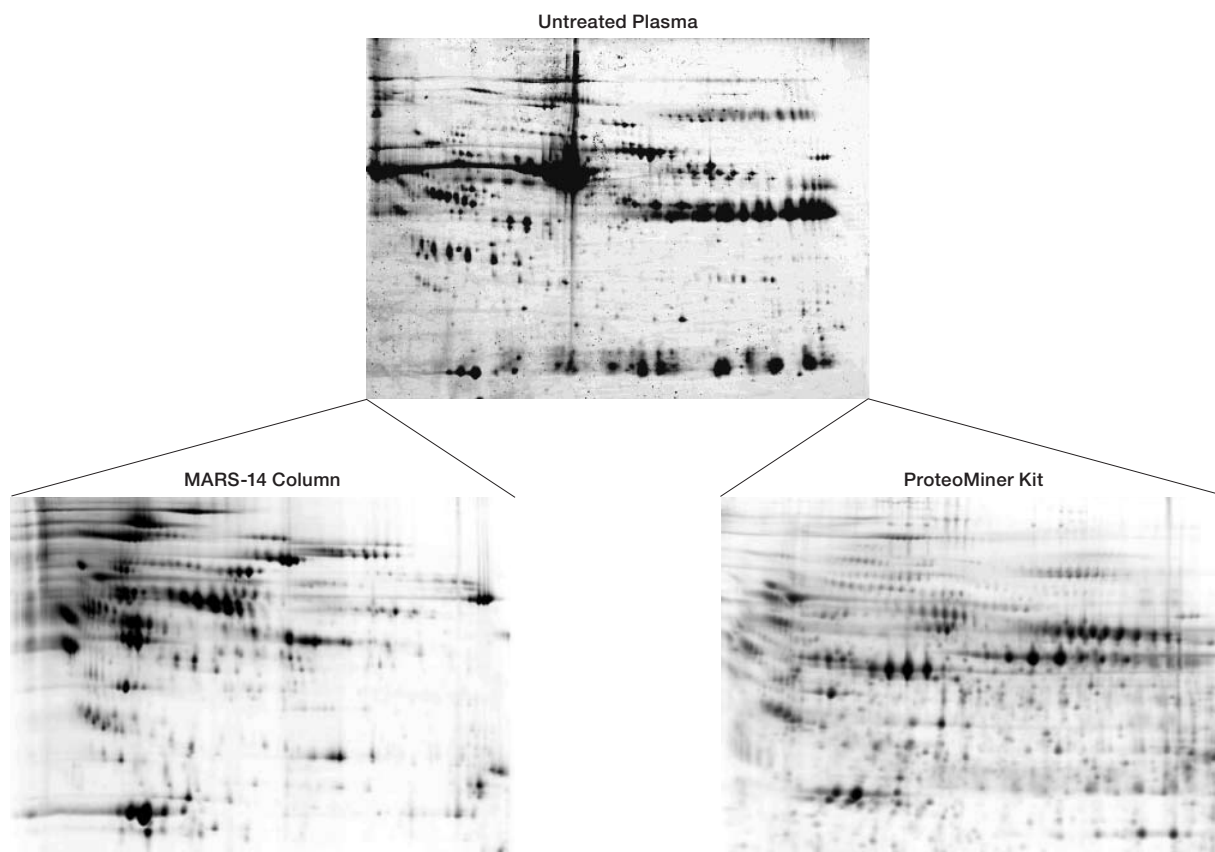


Fig. 2. Comparison of samples before and after treatment with the ProteoMiner protein enrichment kit and an immunodepletion product. Crude plasma along with plasma processed with either the ProteoMiner kit or an Agilent MARS-14 column were analyzed by 2-D electrophoresis. Top, untreated plasma sample; bottom right, ProteoMiner system-treated sample; bottom left, MARS-14 column-treated sample. Substantially more proteins were detected after treatment with the ProteoMiner kit. Data provided by AstraZeneca.

Going Global

Dr Stefan Lehr
Düsseldorf, Germany



Discovering Biomarkers for Diabetes Diagnosis

For more than 30 years at the German Diabetes Center in Düsseldorf, Germany, the latest techniques and research initiatives have merged with patient care to help elucidate all facets of the disease. Research efforts across

various in-house laboratories share the same goals: to gain insights into the physiological mechanisms of the disease, to reduce diabetes-associated complications, and to study and improve patient treatment.

It was this focus on translational research, the movement of discoveries in basic research to application at the clinical level, that induced Dr Stefan Lehr to join the center's research staff after receiving his PhD in biochemistry 8 years ago. Lehr's graduate studies at the University of Cologne had focused on signal transduction and the phosphorylation of insulin receptors, and included identification of specific phosphorylation sites and their physiological role in downstream cellular functions. Experienced in and enthusiastic about using sophisticated laboratory techniques such as mass spectrometry, 2-D gel electrophoresis, and subcellular fractionation, and aware that type 2 diabetes is a disease of increasing prevalence, Lehr established a proteomics lab at the center upon completion of his graduate program.

Today, Lehr continues to use cutting-edge techniques to analyze protein patterns related to type 2 diabetes. One aspect of the proteome lab is analysis of human serum samples to gain insight into the molecular pathogenesis of the disease. One of the challenges Lehr has faced when using techniques such as

2-D differential gel electrophoresis, however, is the interference of high-abundance proteins. "Often the big spots (high-abundance proteins) mask the little spots (specific proteins of interest). Traditional methods for uncovering low-abundance proteins of interest involve several steps, in which you sometimes lose proteins," explains Lehr.

It was this major challenge that prompted Lehr's interest in Bio-Rad's ProteoMiner protein enrichment technology. Since then, Lehr has begun to perform testing with human serum to determine the applicability of this technology to his lab's research. Initial tests with ProteoMiner beads determined that protein profiling with human serum worked according to product manual specifications. Lehr and his team then went on to design experiments now in progress to assess the reproducibility and variability of the technology, as well as its compatibility with methods used in downstream analysis. "The crucial issue in comparative protein profiling is reproducibility," emphasizes Lehr.

With validation now successfully completed, Lehr plans to incorporate ProteoMiner protein enrichment technology into his workflow as a one-step fractionation method for quantitating low-abundance proteins. Ultimately he hopes these efforts will lead to the identification of biomarkers for the early stages of type 2 diabetes. "Frequently, the disease is diagnosed years after onset. During that lengthy period, disease is manifested and time lapses without treatment," says Lehr. He hopes that diagnosing the disease as much as a decade earlier than is currently possible will help prevent complications associated with type 2 diabetes — for example, myocardial infarction and stroke — as well as significantly reduce the costs associated with treatment.

Dr Pier Giorgio Righetti — Combining Science With Imagination

Throughout an illustrious career that began in 1965 with a PhD in chemistry, Dr. Pier Giorgio Righetti has been, as he states, "accused of contaminating science with imagination." Raised by a father who basked in the humanities but struggled to earn a living, Righetti made a deliberate decision toward science, turning his back on perhaps more natural inclinations toward literature and poetry — though not entirely. As he went on to become one of the forefathers of capillary and 2-D electrophoresis, the many papers he published along the way were sprinkled ("contaminated") with literary allusions and metaphors.

But perhaps a hypothesis can be made for imagination as a requirement for scientific discovery — and you only have to trace Righetti's role in the development of ProteoMiner system technology to support this supposition. In 2004, Righetti became aware of Egisto Boschetti's concept to use ligand libraries for affinity-based protein extract treatments. Over the last few years, Righetti and Boschetti have worked together to further the understanding of the molecular mechanisms between libraries and protein extracts, as well as to imagine a number of applications based on the concept of reducing high-abundance while enriching low-abundance proteins in human fluid samples.

Since the proteomics twist on this technology was announced in Siena, Italy, in 2004, Righetti and Boschetti have gone on to publish numerous papers detailing its efficacy. Most recently, they conducted a very fruitful collaborative

research effort to uncover the minority proteome of the red blood cell (98% is hemoglobin; the remaining 2% has been difficult to identify). Published reports have estimated this 2% to be composed of between 91 (Kakhniashvili et al. 2004) and 252 (Pasini et al. 2006) unique proteins. Using ProteoMiner technology, Righetti and Boschetti were able to identify over 1,500 (Figure 3). In true Righetti style, a review discussing these results includes a lengthy prologue metaphorically correlating the search for gold in the proteome with the waves of 49ers migrating into California on a search for gold in the 1800s (Righetti and Boschetti 2008).

When asked to imagine the effect of ProteoMiner system technology, Righetti says that this "first major advancement in proteomics research since the immobilized pH gradient" should have a major impact on the field by enabling:

- Identification of biomarkers for diagnosing pathologies in sera, spinal fluid, saliva, and other human fluids
- Development of drug treatments for diseases based on protein variations
- Identification of previously undiscoverable soluble protein allergens in plant- and animal-based food sources

History has shown that science in general and proteomics in particular, have only benefitted from that which Righetti has been able to imagine.

Dr Jules Westbrook
Dublin, Ireland

The Heart of the Matter



In 1997, proteomics was emerging as a field of study, and Dr Jules Westbrook was earning his bachelor's degree in medical biochemistry at Brunel University in London. Westbrook spent 9 months working with Dr Michael

Dunn at Harefield Hospital, a world-renowned heart and lung transplant center, and that was all it took for him to become convinced that the application of proteomics to cardiovascular disease and heart transplants would revolutionize the understanding and treatment of heart disease. After receiving his degree, Westbrook returned to work in Dunn's lab, joining the transplantation proteomics and neuroproteomics group at the Conway Institute Proteome Research Centre at University College Dublin in Ireland.

The group's main research goals are increased understanding of the molecular processes involved in heart health and disease, and identification of biomarkers that can be used for diagnosis/prognosis or as therapeutic targets. The specific emphasis of the cardiovascular research program is on heart diseases that result in end-stage heart failure, because these are among the leading causes of morbidity and mortality. "For example," explains Westbrook, "we are very interested in dilated cardiomyopathy, or DCM for short, since this is a disease of the heart muscle. As the disease progresses, the heart fails."

The group is particularly concerned with understanding how protein expression is altered in DCM hearts and, by using proteomic techniques to compare normal and diseased hearts, identifying differentially expressed proteins. Human serum, plasma, and tissue samples are the primary source materials used in these projects. According to Westbrook, the masking

of low-abundance by high-abundance proteins is a well-known challenge to extracting meaningful proteomics information relating to a disease or biological process. "Of course, there are many methods available for removing the most abundant proteins from serum or plasma," says Westbrook, "but there is always the risk of losing proteins of potential interest through nonspecific binding interactions."

When Westbrook and his colleagues became aware of the ProteoMiner protein enrichment kit, they were eager to see whether the technology could be used reproducibly to reduce levels of high-abundance proteins without their exclusion (since these might well have significance in disease), yet allow the enrichment of low-abundance proteins. "So far," says Westbrook, "we've tested the kit using human plasma and serum. We're impressed by what we have seen when comparing gel images of untreated samples and samples processed using the ProteoMiner kit."

Results have clearly demonstrated areas of reduction and enrichment, and the reduced areas correspond to the locations where high-abundance proteins migrate. And reproducibility has been confirmed. "We've processed different aliquots of the same samples and produced the same protein profiles on 2-D gels, which is, of course, indicative that the same proteins are being retained to the same degree by the beads," explains Westbrook.

The group is currently following up on initial work by running replicates of treated and untreated human plasma for statistical analysis, and will be using mass spectrometry to attempt to identify the proteins comprising newly visualized spots from enriched and reduced areas. "Looking ahead," says Westbrook, "we think the kit will produce some interesting results when we analyze serum taken from patients with dilated cardiomyopathy. We are very keen to see whether there is enrichment of heart-specific proteins that we know are present."

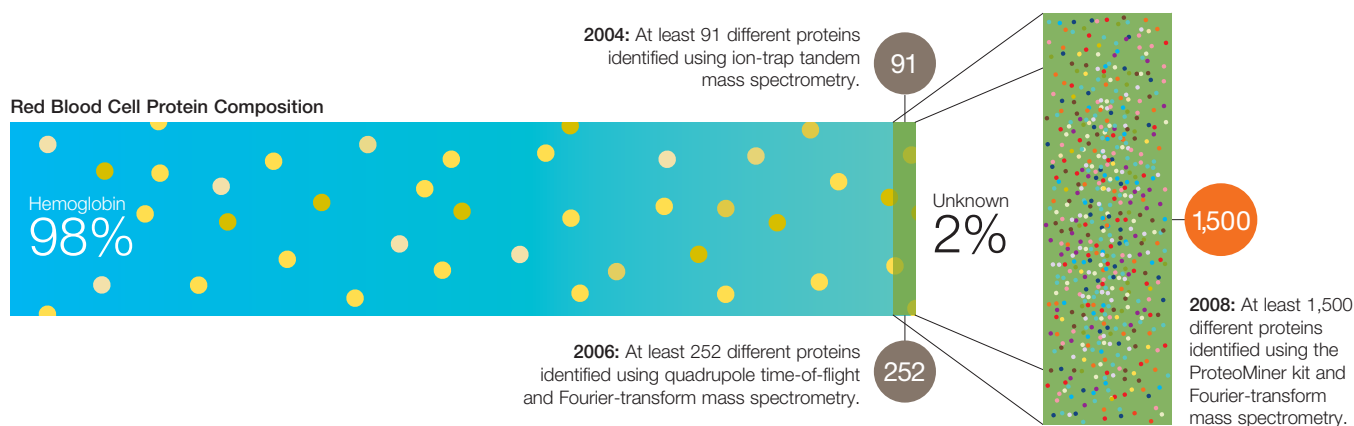


Fig 3. Approximately 98% of the protein composition of a red blood cell is hemoglobin, while the exact protein composition and make up of the remaining (bottom) 2% is unknown, because hemoglobin masks these low-abundance proteins. Analysis of the bottom 2% of proteins between 2004 and 2006 led to estimates of between 91 (Kakhniashvili et al. 2004) and 252 (Pasini et al. 2006) distinct proteins. Recent experiments by Righetti et al. using the ProteoMiner kit led to a revised number of at least 1,500 proteins, a 6-fold increase over previous reports.

Dr Ben Herbert
Sydney, Australia

Exploration Without Boundaries



Ignoring boundaries is not a new concept for Dr Ben Herbert, Director of the Proteomics Technology Centre of Expertise at the University of Technology, Sydney, Australia. In fact, it is a characteristic that can be traced

to the beginning of his career when, fresh out of polytechnic school, he was hired as a lab technician to test sausage content for New Zealand's food industry. This first job and level of education seemed enough for Herbert, until he was asked to help run tests in a study characterizing food proteins. This role sparked an interest in protein separation techniques and led to his pursuit, first of a university degree, and then a PhD in biochemistry. His ability to think outside the box led him initially to commercial ventures, but he was eventually drawn back to academia, where his current role allows him to combine independent thinking with directing scientific research.

Staff scientists are encouraged to ignore traditional boundaries and extend the limits of scientific possibility. "We don't really pay attention to instruction manuals," says Herbert. When Herbert was approached by Bio-Rad to test the ProteoMiner protein enrichment kit, initial tests were conducted using serum and plasma according to manual guidelines. "We do not do a lot of work with serum and plasma," explains Herbert, "so we just tested it and verified that it worked." But the success of these preliminary tests provoked the question, "What else can we use this for?"

A lab conducting research on paralysis ticks became the natural first choice. Found primarily on the eastern coast of Australia, a bite from this tick can cause paralysis and even death in dogs and cats. "In this research, you have to deal with a huge amount of blood from engorged ticks," Herbert explains. Researchers decided to grind up engorged ticks, place the homogenate onto ProteoMiner beads, and work through the

abundant animal proteins present in host blood cells to try to isolate proteins specific to the engorged tick. The ultimate goal is to analyze and identify differences in the protein content of the tick when feeding versus fasting, thereby identifying the proteins causing paralysis.

In another lab at the center, researchers are studying *Cryptococcus gattii*, a potentially fatal lung-infecting fungus. Studies are in progress to compare proteins found in the fungus in its native state with those extracted from infected lung, liver, and kidney samples. Without first processing these tissue samples with ProteoMiner protein enrichment technology, it would be difficult, if not impossible to isolate the fungal proteins from the infected tissue samples. "With the ProteoMiner kit, we can make sure we are not just seeing the top set of animal proteins," says Herbert. "It allows us to remove the animal proteins from the infected organism to uncover those that cause infection."

Perhaps the Proteomics Technology Centre's most boundary-stretching work using ProteoMiner protein enrichment technology concerns the study of cell membrane proteins. Because these proteins are integral to filtering and pumping materials into and out of cells, Herbert believes their characterization will prove crucial to the development of drugs that can be targeted and delivered with precision. There are two major challenges in this area of research, however: membrane proteins are in very low abundance, and they are not as hydrophilic as other types of proteins. According to Herbert, the means for simultaneously analyzing the predicted large numbers of membrane proteins did not exist until ProteoMiner protein enrichment technology. So Herbert and colleagues used the ProteoMiner kit to develop experiments using organic solvents (for example, methanol and trifluoroethanol) to help solubilize and therefore allow the capture of low-abundance membrane proteins. His prediction is that 30% of the low-abundance proteins they are beginning to isolate will be proteins essential to cell membrane permeability.

Conclusions

ProteoMiner protein enrichment technology is being used in laboratories throughout the world to expand what is known about the proteome. It is hoped that the continual discovery of proteins that were previously undetectable because of the dominating presence of high-abundance proteins will lead to the discovery of biomarkers for many debilitating and deadly diseases.

References

- Anderson NL and Anderson NG (2002). The human plasma proteome: history, character, and diagnostic prospects. *Mol Cell Proteomics* 1, 845-867.
- Kakhniashvili DG et al. (2004). The human erythrocyte proteome: analysis by ion trap mass spectrometry. *Mol Cell Proteomics* 3, 501-509.
- Pasini EM et al. (2006). In-depth analysis of the membrane and cytosolic proteome of red blood cells. *Blood* 108, 791-801.
- Righetti PG and Boschetti E (2008). The ProteoMiner and the FortyNiners: searching for gold nuggets in the proteomic arena. *Mass Spec Rev*, in press.
- Sennels L et al. (2007). Proteomic analysis of human blood serum using peptide library beads. *Journ Prot Res* 6, 4,055-4,062.

RNA Quality Indicator: A New Measure of RNA Integrity Reported by the Experion™ Automated Electrophoresis System

Jeff Gingrich, Bio-Rad Laboratories, Inc., Hercules, CA 94547 USA

Introduction

RNA quality plays a major role in the generation of accurate quantitative results from gene expression experiments (Bustin and Nolan 2004). Degraded RNA will not amplify or be labeled to the same degree as intact, undegraded RNA. For many studies, however, the isolation of high-quality RNA is a challenge — particularly from clinical tissue samples that must be handled with extreme care to keep their RNA intact. The determination of RNA quality is therefore a critical initial step in any quantitative gene expression analysis workflow. Yet RNA quality is often assessed by visual inspection of an ethidium bromide-stained agarose gel or skipped if RNA is available only in limited quantities.

The Experion automated electrophoresis system addresses the problems involved in RNA assessment by providing an effective method for determining both the quality and quantity of RNA in a single electrophoresis run. A new feature in Experion software, version 3.0, is a measure of RNA quality called RNA quality indicator (RQI). This novel feature rates RNA quality from 1 to 10, with 10 being the best-quality RNA. In addition, the Experion system can accurately quantitate RNA in a sample: as little as 25 ng of total RNA when the Experion RNA StdSens analysis kit is used, and 200 pg when the Experion RNA HighSens analysis kit is used.

Here we demonstrate the use of RQI to assess RNA quality prior to real-time quantitative PCR (qPCR) experiments. We show that quantitation of RNA using qPCR correlates well with RQI measurements. We propose that RQI can be used as a standardized measure of RNA degradation in a mammalian sample.

Methods

RNA Sample Preparation and Experion System Analysis

Total RNA (1 mg/ml) prepared from the human liver carcinoma cell line HEPG2 was obtained from Ambion, Inc. RNA degradation time courses were performed on RNA diluted to 0.1 mg/ml in TE buffer by incubation at 90°C for up to 7 hr. Aliquots were taken at various times during incubation, and the degree of degradation was assessed by analyzing RNA (50 ng) with the Experion system using the Experion RNA StdSens analysis kit and Experion software, version 3.0, according to kit instructions.

Quantitative Reverse Transcription (RT)-PCR

RNA (500 ng) was converted to cDNA using the iScript™ cDNA synthesis kit. The cDNA (10 ng) was then amplified in triplicate reactions with iQ™ SYBR® Green supermix, and 0.5 μM of each

primer pair for 18S rRNA, and the β-actin, *GAPDH*, *HPRT*, or β-tubulin genes using the iCycler iQ® real-time PCR detection system with version 3.1 software (Gingrich et al. 2006).

Results and Discussion

Assessment of RNA Degradation Using the Experion Electrophoresis System

The RQI feature displays RNA quality assessment results in two convenient, easy-to-understand formats. In one format, RQI rates RNA integrity on a 1 to 10 standardized scale where 1 indicates low-quality (mostly degraded) RNA and 10 indicates high-quality, intact RNA. The RQI of a sample is established by the software comparing the sample electropherogram to a series of degradation standard electropherograms. In the other format, a four-color code is used to label RNA samples based on their quality: green, yellow, and red are used to label high, questionable, and poor RNA qualities, respectively. If a clear (no color) result is shown, the sample could be too dilute to accurately score (<10 ng for the standard-sensitivity assay and <250 pg for the high-sensitivity assay), or the algorithm was unable to evaluate the sample. The color coding is editable and the limits of each region can be adjusted for specific experimental needs.

Preparation of Degraded RNA Samples

Total RNA samples heat-degraded over time were analyzed. As shown in Figure 1A, the size distribution of the smear of RNA decreased as degradation progressed with longer incubation. Concomitant with the decrease in size distribution of the RNA smear, is a decrease in the RQI measurement of the RNA sample starting at an RQI of 9.9 for the undegraded sample. With longer heat incubation and more degradation, the RQI dropped to 1.8 after 5 hr of incubation (Figure 1B).

Relative Quantitation of Degraded RNA in Samples by Real-Time qPCR

To determine the amount of RNA degradation in samples at different time points, qPCR was performed on the RNA samples. In these experiments, primers specific for the 18S rRNA and four selected protein-encoding genes were used in real-time qPCR reactions to quantitate the relative abundance of their respective transcripts at the various time points. The results presented in Figure 2 show that while 18S rRNA appears to have remained mostly intact over the degradation time course, the abundance of the transcripts of the four protein-encoding genes decreased over time.

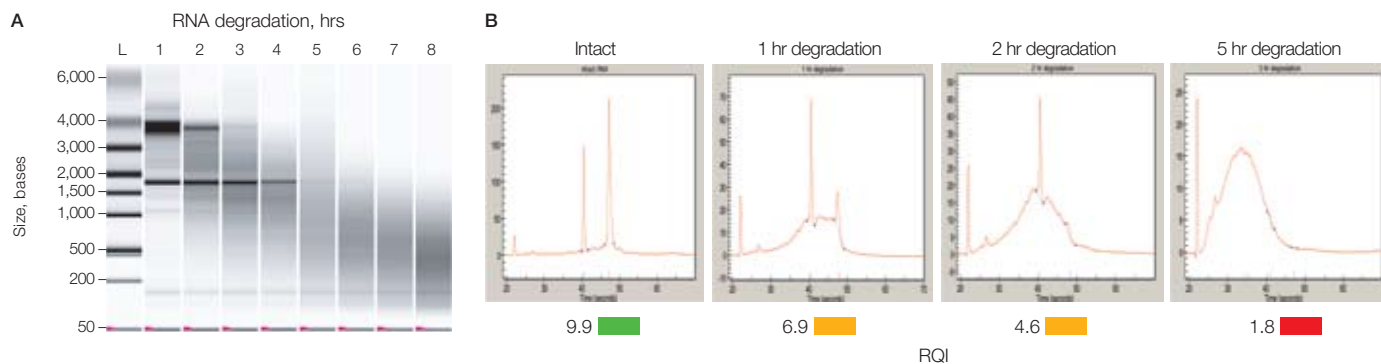


Fig. 1. Time course of degradation of liver carcinoma RNA. Samples of human liver carcinoma total RNA were incubated at 90°C in TE buffer for the times indicated. Aliquots (50 ng) were then separated with the Experion RNA StdSens analysis kit. **A**, simulated gel view showing profiles of the Experion RNA samples at the time points between 0 and 7 hr. L, RNA ladder. **B**, electropherograms of samples collected at selected time points and indicating the RQI. The peak at the far left of the electropherograms corresponds to the lower marker used for alignment of the sample wells.

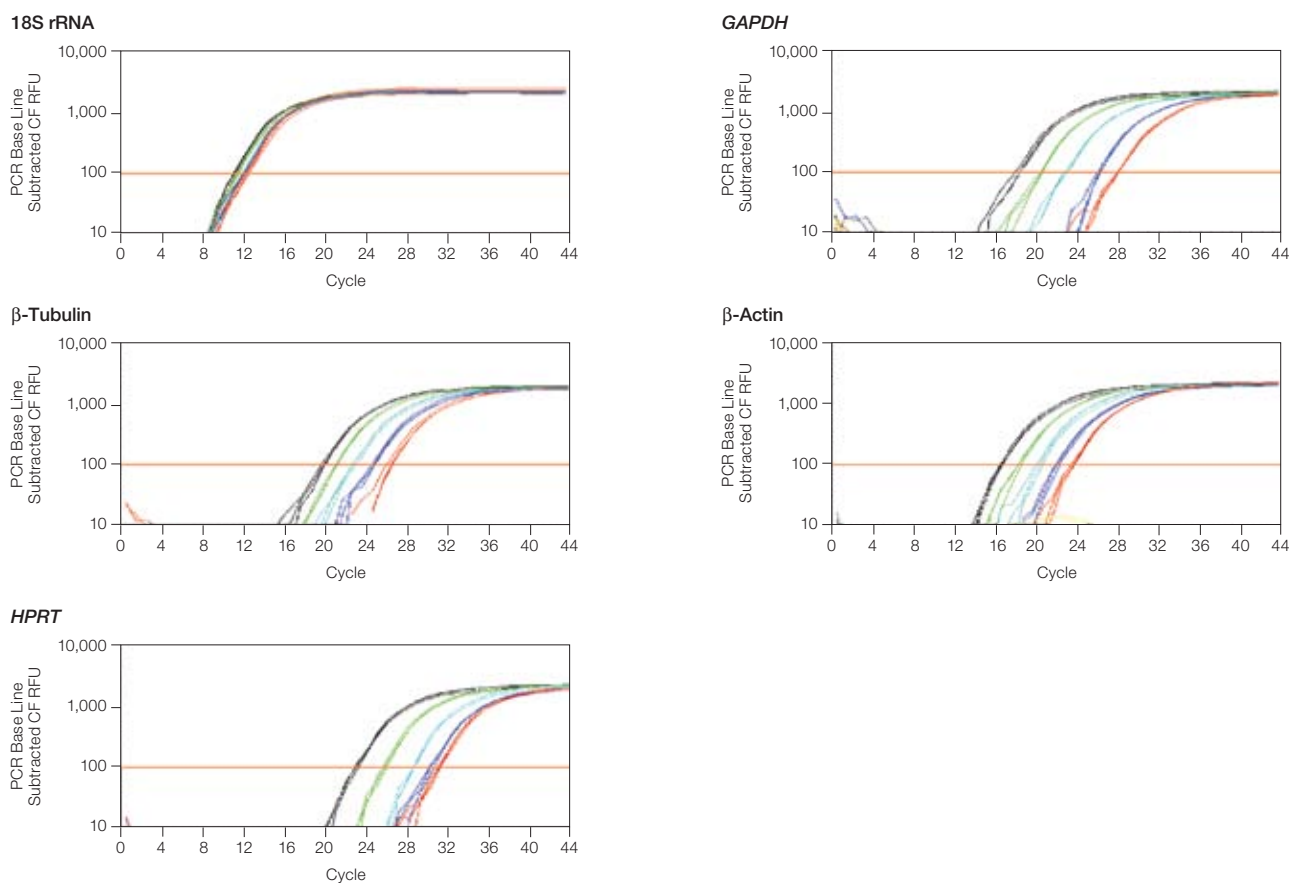


Fig. 2. Assessment of RNA degradation by real-time qPCR. qPCR traces obtained from liver carcinoma total RNA samples degraded for different lengths of time and amplified using primers for the genes indicated. No degradation (—); 1 hr degradation (—); 3 hr degradation (—); 5 hr degradation (—); 7 hr degradation (—). Mean C_T values obtained from these traces are shown in Table 1.

Degradation rates for the protein-encoding gene transcripts are reflected in the increasing threshold cycle (C_T). In real-time qPCR experiments, the C_T number is the number of cycles needed for amplified cDNA fluorescence to pass a set threshold. The C_T number is used to compare the difference in quantity of starting transcript. A difference of one cycle reflects a 2-fold difference in the amount of starting transcript (assuming 100% amplification efficiency). The C_T values of the qPCR reactions from the five gene transcripts are shown in Table 1. The data indicate that the transcripts of the four protein-encoding genes tested were present in different amounts in the initial sample with the β -actin transcript being the most abundant and *HPRT* transcript the least abundant. As expected, transcripts of the 18S rRNA were much more abundant than any of the protein-encoding gene transcripts. Through the 7 hr degradation time, the 18S rRNA was degraded to a much lesser extent than the protein gene transcripts, as seen by a ΔC_T of 1.3, representing a 2.5-fold ($2^{1.3}$) decrease in transcript amount compared to the protein gene transcripts with a ΔC_T of 6.8 to 9.9, representing a 128 to 1,000-fold ($2^{6.8}$ to $2^{9.9}$) decrease in transcript abundance.

Table 1. Impact of RNA degradation on real-time qPCR C_T .*

Incubation time (hr)	C_T					
	RQI	18S rRNA	β -Actin	<i>GAPDH</i>	<i>HPRT</i>	β -Tubulin
0	9.9	11.2	16.5	18.1	22.5	19.7
1	6.9	11.6	18.2	20.5	25.1	20.9
3	3.5	12.0	20.1	22.9	27.9	22.7
5	1.8	12.1	22.0	26.1	29.5	24.6
7	1.5	12.5	23.5	28.0	30.3	26.5
ΔC_T		1.3	7.0	9.9	7.8	6.8

* Real-time qPCR was performed on liver carcinoma RNA samples that were degraded for different lengths of time by incubation at 90°C. Mean C_T values of five transcripts obtained from triplicate reactions were determined at a threshold of 100 relative fluorescence units (RFU) using the iCycler IQ real-time PCR detection system with version 3.1 software. ΔC_T indicates the change in C_T value over the 7 hr degradation period. Traces for the qPCR reactions from which these data were derived are shown in Figure 2.

Correlation of RQI Values With Real-Time qPCR Quantitation of RNA Degradation

In order to correlate the relative amount of remaining RNA of the five different gene transcripts with the measured RQI of the RNA samples, values were plotted as shown in Figure 3. The graph shows that the transcript levels for all five genes decrease logarithmically relative to the RQI measurements down to an RQI value of 3. Below this value, the transcripts decrease at a much faster rate. As mentioned previously, the 18S rRNA transcripts were more abundant and less affected by degradation. The rates of decrease of the four protein-encoding transcripts relative to their RQI measurements were quite similar. Transcripts for *HPRT* and *GAPDH* disappeared slightly faster than those for β -actin and β -tubulin. For example, the transcripts for *HPRT* decreased 10-fold over an RQI range of 4 units, while the transcripts for β -tubulin decreased 10-fold over an RQI range of 7 units.

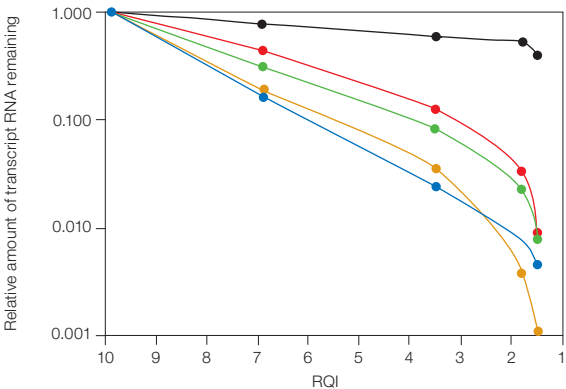


Fig. 3. Correlation between RQI and the relative amount of specific transcript RNA remaining. An arbitrary value of 1 was assigned to the transcript levels corresponding to an RQI of 10. All other values were calculated from the C_T values shown in Table 1, assuming that the number of transcripts is reduced by a factor of 2 for each C_T increase of 1. 18S (◆); Actin (■); GAPDH (▲); HPRT (●); Tubulin (●).

These results demonstrate that RQI measurements can be used to estimate the degree of degradation in an RNA sample. Although we looked at only four protein-encoding genes, they all appeared to degrade to different extents relative to the RQI score. This indicates the need to evaluate RNA degradation states when comparing or performing qPCR to ensure reliable results.

Conclusions

The measurement of degradation is critical to reliable real-time qPCR results. By providing an RQI score, the Experion automated electrophoresis system allows even the most inexperienced user to quickly and effectively quantitate the level of degradation of an RNA sample prior to gene expression analysis.

References

Bustin SA and Nolan T (2004). Pitfalls of quantitative real-time reverse-transcription polymerase chain reaction. *J Biomol Tech* 15, 155-166.
Gingrich J et al. (2006). Effect of RNA degradation on data quality in quantitative PCR and microarray experiments. *Bio-Rad Bulletin* 5452.

Measurement of Caspase-1-Dependent Cytokine Secretion Using the Bio-Plex® Human Cytokine 27-Plex Panel

Martin Keller and Hans-Dietmar Beer, Institute of Cell Biology, Department of Biology, ETH Zurich, CH-8093 Zurich, Switzerland

Introduction

Mammalian cells use the endoplasmic reticulum/Golgi-dependent pathway to export most proteins. However, some proteins are secreted through unconventional, less-understood mechanisms. These proteins include the proinflammatory cytokine prointerleukin-1 β , which requires cleavage by caspase-1 for biological activity and subsequent release.

Several cell types, such as macrophages and keratinocytes, secrete IL-1 β in response to stress signals. For example, UV-irradiation of human keratinocytes activates caspase-1 and thereby induces secretion of IL-1 β (Feldmeyer et al. 2007). We recently published a report indicating that active caspase-1 regulates the unconventional secretion of many additional proteins from keratinocytes and other cell types (Keller et al. 2008).

In this report, we present an RNAi-based method for analyzing caspase-1-dependent release of various cytokines from UV-irradiated human keratinocytes using the Bio-Plex human cytokine 27-plex panel. The panel includes IL-1 β in addition to 26 other cytokines, 21 of which (Table 1) possess a signal peptide. This allowed us to determine whether caspase-1 specifically targets unconventional protein secretion or secretion in general.

Methods

Cultivation and siRNA Transfection of Keratinocytes

Primary human keratinocytes were isolated from the foreskin of a 3-year-old donor as previously described (Rheinwald and Green 1975). Cells were grown as adherent cultures in keratinocyte-SFM growth medium (Gibco Invitrogen Corporation) and supplemented with epidermal growth factor (EGF) and bovine pituitary extract (BPE) provided by the medium supplier.

siRNA transfection has been previously described (Keller et al. 2008). In brief, keratinocytes were seeded into 14 cm dishes (4.5×10^6 cells per dish). After one day, the cells were transfected with 21-mer duplex siRNAs (Sigma-Aldrich Co.) specific for caspase-1 or vascular endothelial growth factor (VEGF). Target sequences used for caspase-1 were GGCAGAGAUUUUAUCCAUAUATT or CCAAUAAUGGACAAGUCA, and sequences for VEGF were CUGAUGAGAUUCGAGUACAUTT or UGUGAAUGCAGACCAAAGATT. INTERFERin (Polyplus-transfection SA) was used as the transfection reagent according to the manufacturer's instructions, and the final transfecting siRNA concentration was 50 nM. Reduction of target gene expression was determined by real-time PCR and western blotting using β -actin as an internal reference (data not shown).

Stimulation of Protein Secretion and Sample Preparation

After siRNA transfection (48 hr, or 24 hr after seeding untransfected cells), cells were washed three times with PBS and 5 ml of fresh medium per dish (without growth supplement) was added. After 1 hr, cells were irradiated with 50 mJ/cm² UVB. The supernatant was removed 4 hr after irradiation, and adherent plus pelleted cells from the supernatant were lysed for 10 min in 1 ml of PBS containing 2% Triton X-100 per dish. The lysed cells were diluted to 5 ml in growth medium and cellular debris was removed by low-speed centrifugation. Both cell culture supernatants and cell lysates were snap frozen and stored at -70°C until analysis. Lactate dehydrogenase (LDH) activity was measured by the CytoTox 96 nonradioactive cytotoxicity assay (Promega Corporation).

Multiplex Bead Suspension Array and Data Evaluation

Cytokine concentrations in cell lysates (Lys) and supernatants (SN) were determined using the Bio-Plex multiplex bead-based suspension array system with the human cytokine 27-plex panel (Table 1). Analysis and data processing were performed according to system and panel instructions. Values below the dynamic range of the assay were set to zero and the corresponding cytokines were not included in the figures. Total protein expression levels were calculated using the formula: (Lys + SN) and the percent of cytokine release from the cells was calculated according to the formula: SN/(Lys + SN).

Table 1. Bio-Plex human cytokine 27-plex panel.

IL-1 β *	Basic FGF-2*
IL-1ra*	Eotaxin*
IL-2	G-CSF*
IL-4	GM-CSF*
IL-5	IFN- γ *
IL-6*	IP-10*
IL-7*	MCP-1*
IL-8*	MIP-1 α *
IL-9*	MIP-1 β
IL-10	PDGF-BB*
IL-12 (p70)*	RANTES
IL-13*	TNF- α *
IL-15*	VEGF*
IL-17*	

*Cytokine known to be secreted by keratinocytes.

Results and Discussion

We first determined which cytokines were secreted by keratinocytes upon UVB irradiation. Supernatants from cells 4 hr after irradiation or from unirradiated cells were collected and analyzed using the human cytokine 27-plex panel. For the UVB-irradiated keratinocytes, 21 out of 27 cytokines measured in the panel were detected in the supernatant (Table 1, Figure 1). Most of these cytokines are known to be produced by keratinocytes. IL-2, IL-4, IL-5, IL-10, macrophage inflammatory protein (MIP)-1 β , and RANTES could not be detected in the supernatants. These cytokines, which are normally not produced by keratinocytes, can be used as negative controls to verify the validity of the measurement.

As expected, secretion of IL-1 β was enhanced by UV-irradiation (more than 3-fold). The same stimulus also induced the export of IL-7 (nearly 3-fold) and to a lesser extent of eotaxin, platelet-derived growth factor (PDGF), and tumor necrosis factor (TNF)- α . TNF- α expression is known to be induced by IL-1 β , and UV-irradiation therefore most likely enhances TNF- α release indirectly via IL-1 β .

In order to determine the impact of caspase-1 expression on cytokine secretion, we transfected human primary keratinocytes with siRNA and thereby reduced caspase-1 expression. Suppression of VEGF expression served as a control. Knockdown efficiencies were demonstrated in recent publications (Feldmeyer et al. 2007, Keller et al. 2008). Protein expression of caspase-1 was reduced to approximately 20% of its normal expression levels.

UV irradiation leads to some degree of protein release because of cell lysis. In order to quantitate the impact of UV on cell lysis, we measured extracellular versus total activity of the cytoplasmic enzyme LDH (Figure 2). Based on these measurements, the degree of lysis due to irradiation was about 7% (+UV). Cell lysis of caspase-1 siRNA-transfected cells did not differ more than 2% from VEGF siRNA-transfected cells.

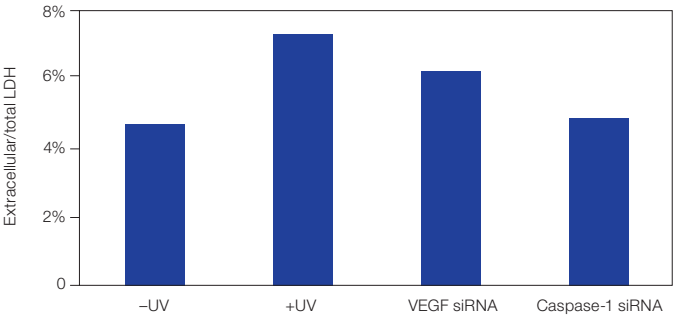


Fig. 2. Assessment of cell lysis by LDH activity measurement. The degree of cell lysis in experiments described in Figures 1 and 3 were determined by measuring extracellular versus total activity of the cytoplasmic enzyme LDH.

Therefore, apparent differences in cytokine concentrations in the supernatant are not expected to be due to UV-induced cell lysis.

To analyze the influence of caspase-1 on both cytokine expression and secretion, we analyzed cell lysates and supernatants using the human cytokine 27-plex panel (Figure 3). This allowed us to observe that knockdown of caspase-1 did not change the expression of most cytokines (Figure 3, upper panel).

Cytokine levels from the cell lysate and the supernatant (Figure 3, middle panel) can be used to calculate the percentage of cytokine released by the cells (Figure 3, lower panel). As expected, siRNA-mediated knockdown of caspase-1 leads to a 3-fold reduction of IL-1 β secretion after UVB irradiation. Additionally, secretion of IL-1 α , IL-17, granulocyte-macrophage colony-stimulating factor (GM-CSF), interferon (IFN)- γ , MIP-1 α , and TNF- α were also reduced by caspase-1 downregulation, however, to a much lower extent. Expression and therefore secretion of several of these proteins are induced indirectly via IL-1 β and are therefore only indirectly mediated by caspase-1.

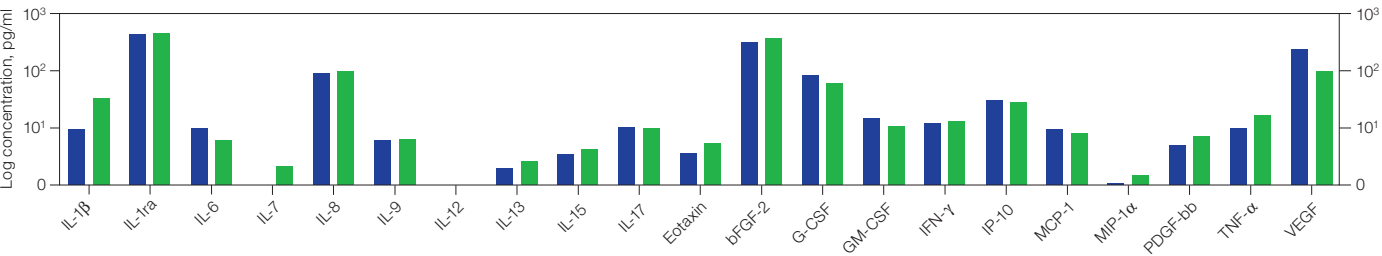
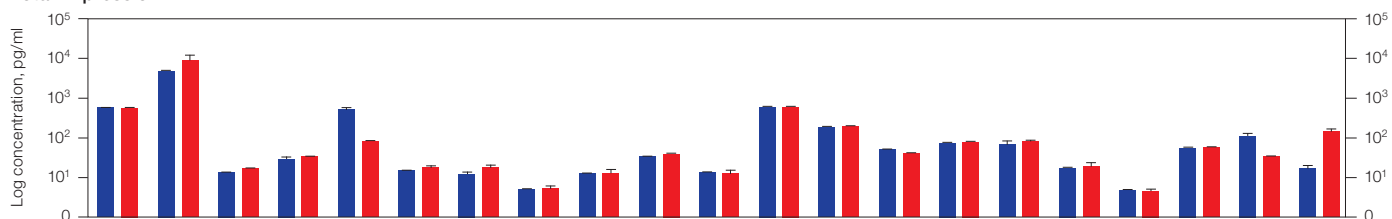
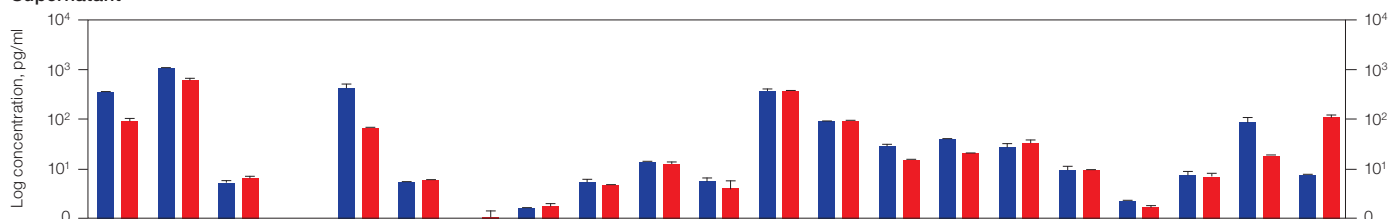


Fig. 1. UVB-induced cytokine secretion from keratinocytes. Cytokines were measured in cell culture supernatants from keratinocytes 4 hr after UVB irradiation (■) or in control cells (■) using the Bio-Plex multiplex array system and human cytokine 27-plex panel. Bars represent values from single measurements. The 21 cytokines found to be secreted are shown.

Total Expression



Supernatant



Percentage Secretion

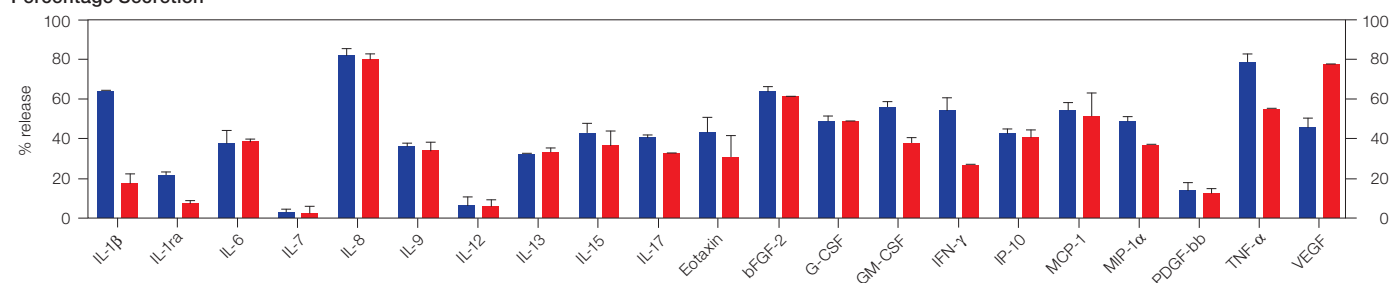


Fig. 3. Caspase-1-dependent cytokine expression and secretion of keratinocytes after UVB irradiation. Cytokines were measured in cell culture supernatants and cell lysates 4 hr after irradiation of keratinocytes transfected with siRNA specific for caspase-1 (■) or VEGF (■) using the Bio-Plex multiplex array system and human cytokine 27-plex panel. Bars represent mean \pm standard deviation of values obtained from two different siRNA target sequences per gene.

Conclusions

Multiplex cytokine suspension array technology is a powerful tool for identifying cytokines that are secreted from cells under certain conditions. The advantage of this method is the concomitant quantitative measurement of several cytokines from different samples of the same experiment.

With our strategy, we could verify that in keratinocytes, caspase-1 only affects unconventional protein secretion and not protein expression in general. Our results show that it is critical to measure cytokine concentrations in both supernatant and cell lysate. This allows the calculations of percentages of secretion, thereby accounting for changes in protein expression.

Our approach can be applied to virtually all cell types that can be cultured, and even to tissue cultures. siRNA, specific inhibitors, and knockdown cells can then be used to investigate the impact of genes or cellular processes on protein secretion.

References

- Feldmeyer L et al. (2007). The inflammasome mediates UVB-induced activation and secretion of interleukin-1 β by keratinocytes. *Curr Biol* 17, 1140-1145.
- Keller M et al. (2008). Active caspase-1 is a regulator of unconventional protein secretion. *Cell* 132, 818-831.
- Rheinwald JG and Green H (1975). Serial cultivation of strains of human epidermal keratinocytes: the formation of keratinizing colonies from single cells. *Cell* 6, 331-343.

Contact information: Martin Keller, PhD, Institute of Cell Biology, Department of Biology, ETH Zurich, CH-8093 Zurich, Switzerland

A Simple Protocol to Insert the Profinity eXact™ Tag Into Alternate Expression Vectors

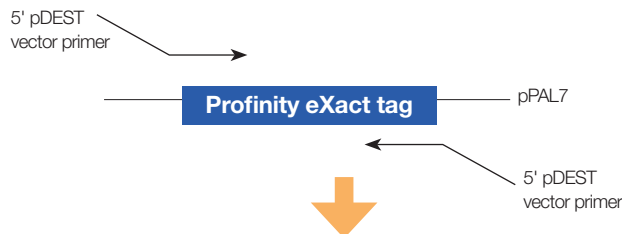
Introduction

The Profinity eXact affinity purification system yields purified, tag-free target protein in as little as 1 hour after lysate loading. This system utilizes an immobilized mutant subtilisin protease that binds the Profinity eXact tag with high affinity; upon addition of a fluoride-containing elution buffer, the protease is activated and the tag-free target protein is quickly released. The Profinity eXact tag is expressed as an N-terminal tag and contains an engineered cleavage recognition sequence (EEDKLFKAL) at its C-terminus. Cleavage occurs directly after this sequence. The majority of proteins are purified without any residual amino acids from the Profinity eXact tag. However, if cysteine or proline immediately follows the cleavage recognition site, cloning should be performed to introduce a two-amino-acid spacer (Thr-Ser) prior to the starting amino acids of the target protein of interest. *E. coli* expression of a Profinity eXact fusion protein is easily accomplished with the Bio-Rad pPAL7 expression vector, which facilitates construction of an N-terminal Profinity eXact fusion tag with the protein expressed by the target DNA sequence. However, some users prefer to use other expression vectors in order to utilize alternative promoters, selection markers, or C-terminal affinity tags.

This article describes one method that can be used to quickly clone the Profinity eXact tag into a different expression vector. First, a PCR fragment containing the Profinity eXact tag is created with 5' and 3' sequences complementary to the insertion site of the expression vector to be modified. The two strands of the PCR fragment are then used as mutagenesis oligonucleotides to insert the new affinity tag into the expression vector or replace undesired sequences (for example, 6xHis tag) with the Profinity eXact tag. A modification of the manufacturer's instructions for the QuikChange XL site-directed mutagenesis kit (Stratagene Corporation) is used to create DNA sequences of up to 1 kb for insertion (Geiser et al. 2001). The example illustrated in this article describes the substitution of the Profinity eXact tag for the 6xHis tag within the Gateway pDEST17 vector (Invitrogen Corporation) (Figure 1).

Step 1: Design Primers

Primers are designed to produce the Profinity eXact tag with 5' ends that are complementary to the flanking regions of the insertion/substitution site.



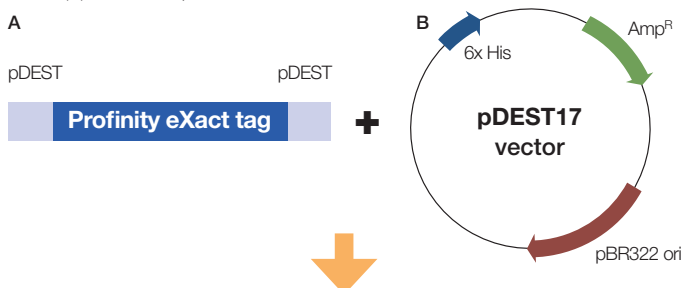
Step 2: Perform PCR

The resultant double-stranded PCR fragment is used as oligos for the mutagenesis reaction.



Step 3: Perform Mutagenesis

During the mutagenesis reaction, the Profinity eXact tag (A) replaces the original 6x His (B) used in the pDEST17 vector.



Step 4: Create Modified pDEST17 Vector

The pDEST17 vector containing the Profinity eXact tag is created.

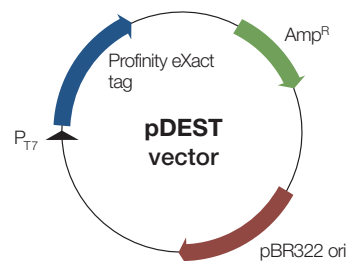


Fig. 1. Outline of strategy to replace 6xHis tag of Gateway pDEST17 recipient vector with the Profinity eXact tag.

Profinity eXact Tag Cloning Protocol

Use this method to insert the Profinity eXact tag into any expression vector quickly and easily:

1. Use PCR to create the oligonucleotide fragments needed for use with the QuikChange XL site-directed mutagenesis kit (The fragments are too long — greater than 250 bases — for chemical synthesis).

Figure 2 shows the primers containing the Profinity eXact tag (red sequences) flanked by the DNA sequences complementary to the region surrounding the pDEST17 insertion/replacement site (blue and green sequences in Figures 2 and 3).

Forward primer 5' GAAATAATTTGTTTAACTTTAAGAAGGAGATATACATATG

GGAGGGAATCAACGGG

Reverse primer 5' CATTTTACGTTTCTCGTTCAGCTTTTGTACAACTTGT

CAAAGCTTTGAAGAGCTTGTG

PCR conditions

ddH₂O 34.5 µl

10× Pfu reaction buffer 5.0 µl

dNTP 1.0 µl

pPAL7 (100 ng/µl) 0.5 µl

Forward primer (10 µl) 4.0 µl

Reverse primer (10 µl) 4.0 µl

Pfu polymerase (1 U/µl) 1.0 µl

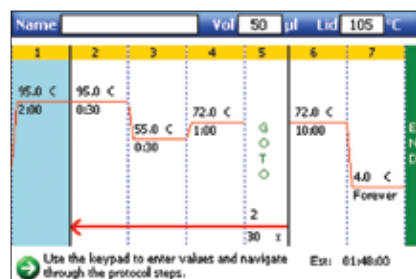


Fig. 2. Primer design and PCR setup to create mutagenesis oligos.

T7 promoter	
1	AGATCTCGAT CCCGCGAAT TAATACGACT CACTATAGG AGACCACAAC GGTTCCTCTC TCTAGAGCTA GGGCGCTTA ATTATGCTGA GTGATATCCC TCTGGTGTG CCAAAGGGAG
initiation ATG	
	NdeI 6xHis
61	TAGAAATAAT TTGTTTAACT TTTAAGAAGG AGATATACAT ATGTCGTACT ACCATCACCA ATCTTTATTA AACAAATTG AATTTCTTCC TCTATATGTA TACAGCATGA TGGTAGTGGT
6xHis attR1	
121	TCACCATCAC CTCGAATCAA CAAGTTTGTA CAAAAAAGCT GAACGAGAAA CGTAAATGA AGTGGTAGTG GAGCTTAGT GTTCAACAT GTTTTTTCGA CTTGCTCTTT GCATTTTACT
attR1	
181	TATAAATATC AATATATTAA ATTAGATTTT GCATAAAAA CAGACTACAT AATACTGTAA ATATTTATAG TTATATAATT TAATCTAAAA CGTATTTTTT GTCTGATGTA TTATGACATT
attR1	
241	AACACAACAT TCCAGTCAC TATGGCGGCC GCATTAGGCA CCCCAGGCTT TACACTTTAT TTGTGTTGTA TAGGTCAGTG ATACCGCCGG CGTAATCCGT GGGGTCCGAA ATGTGAAATA

Fig. 3. Target pDEST17 vector DNA sequence. The region highlighted in blue represents the sequence that should be present on the 5'-end of the Profinity eXact forward primer. The region highlighted in green represents the sequence that should be present on the 5'-end of the Profinity eXact reverse primer. After the QuikChange XL mutagenesis kit reaction, the insertion site highlighted in yellow will be replaced by the Profinity eXact tag.

2. Purify the PCR product using a 1% ReadyAgarose™ gel. Figure 3 shows the complementary regions along with the insertion site in the pDEST17 vector DNA sequence.
3. Modify the pDEST17 vector using the QuikChange XL site-directed mutagenesis kit with the conditions illustrated in Figure 4.

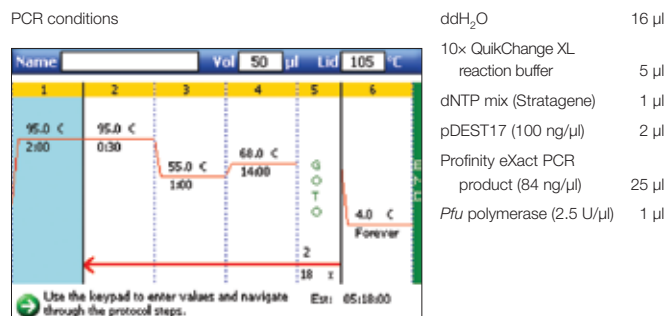


Fig. 4. Mutagenesis reaction to create pDEST17 vector modification.

4. Treat the resulting PCR product with DpnI as described in the QuikChange XL protocol.
5. Use the DpnI-treated PCR product (5 µl) to transform *E. coli* cloning chemi-competent cells (50 µl, Bio-Rad catalog #156-3000).
6. Culture the putative transformant colonies.
7. Isolate the Profinity eXact tag-pDEST vector using mini prep DNA purification.

Summary

Benefits of using the Profinity eXact fusion tag system include time savings, increased lab efficiency, and the ability to generate unadulterated, tag-free protein in under an hour. The ability to obtain a purified target protein, free of its fusion partner, may still be realized regardless of its use with the pPAL7 expression vector. Whether due to user preference or increased familiarity with other expression vectors, there remain certain impediments for researchers when it comes to adoption of a new cloning system. The example presented here demonstrates how the Profinity eXact tag can easily be used to replace another tag (for example, 6x His) by being inserted into a non-pPAL expression vector of choice. Depending on the vector to be modified, the user may instead choose to perform restriction enzyme cloning or recombination-mediated techniques, both common alternative strategies for DNA manipulation.

Reference

Geiser M et al. (2001). Integration of PCR fragments at any specific site within cloning vectors without the use of restriction enzymes and DNA ligase. *Biotechniques* 31, 88-90, 92.

Gaining Insight Into Inflammatory Response Pathways



Beneath the Rocks of Inflammation

Self-described as the kind of child who turned over rocks and spent hours studying what he found underneath, Dr Ulrich Schaff currently applies this passionate curiosity to the study of inflammation and its relationship to chronic medical conditions.

Although the inclination toward discovery came naturally, an interest in the “wet” side of science was not such a given. Schaff was one of the first students in the undergraduate bioengineering program at UC Berkeley. His major interest was the application of engineering to the study of fluidics and fluid dynamics. Schaff began graduate work in the same field at UC Davis in Dr Scott Simon’s laboratory, where research focuses on neutrophils, monocytes, and occasionally T cells. Initially, Schaff applied his engineering acumen to designing a microfluidics system that simulates small blood vessels. Shortly thereafter, however, his interests began to shift. Schaff became involved in a project investigating cellular and molecular mechanisms relating to the role that cell-surface adhesion molecules play in activating leukocytes (specifically neutrophils, Figure 1) during the inflammatory response to infection. Neutrophils are the first leukocytes recruited during the initial phase of the inflammatory response. Excessive recruitment of neutrophils may be associated with debilitating — even life threatening — conditions such as autoimmune and chronic inflammatory lung diseases.

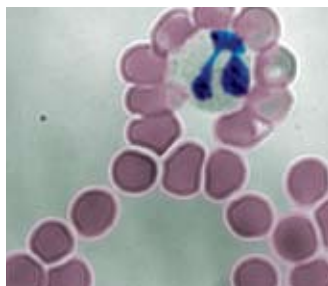


Fig. 1. Neutrophil in whole blood identified by multi-lobed appearance of its nucleus after staining. Although neutrophils are the most common circulating white blood cells, they are outnumbered more than 1,000:1 by red blood cells. Because neutrophils hunt down and engulf bacteria, a high neutrophil count often signals bacterial infection.

The main focus of Schaff’s graduate studies was the first step in this cellular inflammatory response pathway, when neutrophils roll and adhere to the endothelial lining of the blood vessel prior to transmigration into infected tissue. Near the end of his studies, Schaff began to focus on a particular calcium channel protein that had been recently discovered in T cells (Feske et al. 2006). This protein also seems to play a key role in activating leukocyte-endothelium adhesion during inflammation. At the time he heard about this discovery, Schaff had been imaging intracellular calcium in neutrophils during inflammation using his microfluidic devices.

He wondered whether neutrophil and T cell calcium channel signalling were related. Ultimately, it was the intrigue of this calcium channel-related research that solidified his decision to continue as a postdoctoral scientist with the Simon lab rather than pursue an engineering career in the private sector.

Specificity Is Key to Discovery

“The reason you focus on something specific when studying the inflammatory response, such as a calcium channel,” explains Schaff, “is because if anti-inflammatory drugs are targeted at something more widely distributed throughout multiple cell types, such as a chemokine receptor, the side effects can be crippling to nontarget cells.”

Calcium signals are universal regulators of cellular responses. Intracellular calcium flux — the rapid rise in calcium concentration inside a neutrophil when it senses bacteria — is integral to the recruitment phenomenon in neutrophils. The Simon lab was able to determine that at least one store-operated calcium channel — protein that opens when internal stores of calcium are empty — is involved in the calcium flux in neutrophils. Their research findings indicated that bacterial products bind to chemical sensors on the neutrophil, causing calcium to be released from stores inside the cells. This emptying of the stores signals the store-operated calcium channel to open up as well (Figure 2). The challenge became identifying this calcium channel. “Colleagues suggested that the ORAI1 transmembrane protein described in a recent *Nature* article by Feske, a protein discovery that has flung open the field of store-operating calcium research in the T cell world, might be related to this phenomenon in neutrophils,” says Schaff.

Need for an Electroporation System

To isolate the ORAI1 protein as the channel involved in neutrophil calcium flux, Schaff initially conducted experiments with chemical inhibitors of calcium flux, as well as ions known to block ORAI1 channels, and observed that neutrophils were prevented from arresting and migrating in response to inflamed endothelial cells. In addition, inducing store-operated calcium flux caused neutrophils to arrest and migrate in the absence of normal inflammatory stimulus. What could not be determined, however, was whether these phenomena were due to the activity of ORAI1 or another unknown calcium channel. The only way to study the ORAI1 protein with any degree of specificity seemed to be via genetic manipulations. “We were told by researchers studying T cells, that because ORAI1 has only been known of for a short time, siRNA and overtransfecting are the only ways to study it,” says Schaff. “Our lab simply was not set up to do this type of work.”

Schaff searched the literature and learned that almost all transfections of leukocytes are done by electroporation; a leukocyte has a small surface area compared to its volume, so electroporation is the best way to get nucleic acids into the

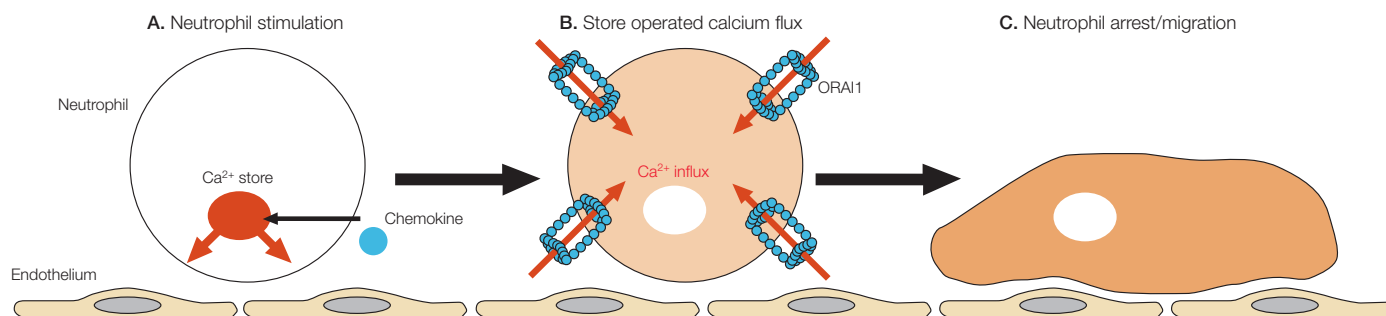


Fig. 2. Calcium influx through a store-operated calcium channel controls neutrophil activation. **A**, inflammatory chemokine from the blood vessel endothelium causes a rolling neutrophil to release internal stores of calcium. **B**, emptying of the stores causes the calcium channel to open calcium selective pores in the membrane, resulting in influx of calcium. **C**, elevation of cytoplasmic calcium signals the neutrophil to stop rolling (arrest), change shape, and migrate toward bacteria or other sources of inflammation. Experimentation using the Gene Pulser MXcell electroporation system helped identify the ORAI1 protein as the calcium channel involved in this phenomenon. In summary, ORAI1 is the store-operated calcium channel that opens when internal stores of calcium are empty. As a transmembrane protein, ORAI1 forms pores that selectively let calcium into the cell and can open or close in response to the amount of calcium in the internal stores. When ORAI1 opens, large amounts of calcium move into the cell.

cytoplasm or nucleus. To continue their research, the Simon lab needed an electroporator that works with difficult-to-transfect cell lines and yields highly specific transfection results.

At about the same time, Bio-Rad contacted UC Davis's technology transfer center — a center that pairs commercial entities with university laboratories — to find research partners for the Gene Pulser MXcell™ electroporation system (Figure 3). Several labs were identified as potential partners, including the Simon lab. “We were looking to develop a collaboration with researchers working with primary cells. The Simon lab was chosen because they’ve experienced technical roadblocks and seemed excited about the opportunities electroporation would bring to their research,” says Bio-Rad product manager Michelle Collins.



Fig. 3. Gene Pulser MXcell electroporation system.

Role of the Gene Pulser MXcell Electroporation System

Schaff's studies use the HL60 cell line, a line of neutrophil progenitor cells. The cells are differentiated by addition of DMSO to the medium, causing them to divide and become smaller. Because these cells are notoriously difficult to transfect, Schaff started experimenting with the Gene Pulser MXcell system first by conducting studies to determine optimal waveform. Schaff reports, “We got better survival and results with the exponential function.” The system allowed them to quickly optimize capacitance, voltage, concentration of transfecting RNA, and cell survival and response to increasing incubation times with RNA.

After optimization, the Simon lab began defining the role of the ORAI1 protein in the inflammatory response. “We have conducted many different assays to determine the functional importance of ORAI1,” says Schaff. Among them are knockdown studies of the

protein to reduce several phenotypes associated with neutrophil activation when the chemokine is added. Initial results have shown a correlating decrease in cell arrest and calcium flux in the cells.

“None of these studies,” says Schaff, “would have been possible without this electroporation device.”

Effect on Future Research

“We have found the Gene Pulser MXcell system to offer a very simple technique that is especially beneficial for difficult-to-transfect cells,” says Schaff. “We can produce a constant stream of transfected cells, which is very useful, especially since they’re scalable batches of cells — just add or subtract wells.”

Future plans of the Simon lab include studying ORAI1 functionality through electroporation of inhibitory peptides. Since peptides need to be injected into the cell through microinjection or some other technique that opens holes in the cell membrane, the Gene Pulser MXcell system seems ideal for this purpose. “We also have begun to transfect neutrophils with *ORAI1*-expressing plasmids,” says Schaff. A primary cell line, neutrophils are very difficult to work with because they only live about 24 hours outside the body, so they are performing transient transfections.

It is hoped that these efforts will help determine methods for suppressing the neutrophil recruitment response. “For instance,” says Schaff, “if the calcium channel turns out to be a significant part of the adhesion cascade, an inhibitor can be developed against the calcium channel.”

It would seem that the “rocks” that comprise inflammatory-related diseases provide Schaff with an outlet for investigating what’s “underneath”: neutrophils, calcium channels, and the ORAI1 protein. Hopefully in the process, the harmful effects of diseases related to the inflammation response, such as autoimmune and chronic inflammatory lung diseases, will be greatly reduced, if not eliminated.

Reference

Feske et al. (2006). A mutation in ORAI1 causes immune deficiency by abrogating CRAC channel function, *Nature*, 179–185.

Sample Quantitation

- 5693 Measurement of low-volume DNA samples using the Hellma TrayCell fiber-optic device with the SmartSpec™ Plus spectrophotometer

Chromatography

- 5744 Profinia™ buffers for *Strep*-tag protein chromatography product information sheet
- 5742 Profinity eXact™ purification methods on the Profinia system product information sheet
- 5741 Profinia buffers for maltose-binding protein (MBP) chromatography product information sheet
- 5725 Profinia buffers for Profinity eXact chromatography product information sheet
- 5712 Profinia protein purification system simplifies antibody purification with protein A

Process Chromatography

- 5739 CHT™ ceramic hydroxypatite using a Bio-Rad® InPlace™ column
- 5735 Purification of a monoclonal antibody using a combination of UNOsphere™ *rapid S* and UNOsphere Q media ion exchange chromatography after protein A capture
- 5734 UNOsphere *rapid S* media product information sheet
- 5662 Process chromatography applications laboratory brochure

Automated Electrophoresis

- 5732 Experion™ Pro260 and RNA StdSens starter kits product information sheet

Electrophoresis and Blotting: Apparatus

- 5479 DCode™ system CD-ROM

Imaging

- 5723 Increased western blot throughput with multiplex fluorescent detection

Multiplex Suspension Array Technology

- 5649 Development and validation of a novel multiplex immunoglobulin isotyping assay on magnetic microspheres

Gene Transfer

- 5733 Transfection of Chinese hamster ovary-derived DG44 cells using the Gene Pulser MXcell™ electroporation system
- 5720 Transfection of neuroblastoma cell lines using the Gene Pulser MXcell electroporation system
- 5700 Gene Pulser MXcell electroporation guide

Amplification/PCR

- 5737 iTaq™ fast supermixes with ROX for qPCR flier

Legal Notices

Autoflex is a trademark of Bruker Daltronik GmbH. DyNA Quant is a trademark of Hoefer Inc. Excel is a trademark of Microsoft Corporation. Hoechst 33258 and Microcapillary Drummond pipets are trademarks of Sigma-Aldrich Company. MagPlex and MicroPlex are trademarks of Luminex Corporation. P2 Pipetman is a trademark of Gilson Incorporated. PicoGreen and SYBR Green are trademarks of Invitrogen Corporation. QuickChange is a trademark of Stratagene Corporation.



LabChip and the LabChip logo are trademarks of Caliper Life Sciences, Inc. Bio-Rad Laboratories, Inc. is licensed by Caliper Life Sciences, Inc. to sell products using the LabChip technology for research use only. These products are licensed under US patents 5,863,753, 5,658,751, 5,436,134, and 5,582,977, and pending patent applications, and related foreign patents, for internal research and development use only in detecting, quantitating, and sizing macromolecules, in combination with microfluidics, where internal research and development use expressly excludes the use of this product for providing medical, diagnostic, or any other testing, analysis, or screening services, or providing clinical information or clinical analysis, in any event in return for compensation by an unrelated party. The Bio-Plex suspension array system includes fluorescently labeled microspheres and instrumentation licensed to Bio-Rad Laboratories, Inc. by the Luminex Corporation. Purification and preparation of fusion proteins and affinity peptides containing at least two adjacent histidine residues may require a license under US patents 5,284,933 and 5,310,663, including foreign patents (assignee: Hoffmann-La Roche). Purchase of Criterion XT Bis-Tris gels, XT MOPS running buffer, XT MES running buffer, XT MOPS buffer kit, and XT MES buffer kit is accompanied by a limited license under US patents 6,143,154; 6,096,182; 6,059,948; 5,578,180; 5,922,185; 6,162,338; and 6,783,651 and corresponding foreign patents. The SELDI process is covered by US patents 5,719,060, 6,225,047, 6,579,719, and 6,818,411 and other issued patents and pending applications in the US and other jurisdictions. Profinity eXact vectors, tags, and resins are exclusively licensed under patent rights of Potomac Affinity Proteins. This product is intended for research purposes only. For commercial applications or manufacturing using these products, commercial licenses can be obtained by contacting the Life Science Group Chromatography Marketing Manager, Bio-Rad Laboratories, Inc., 6000 Alfred Nobel Drive, Hercules, CA 94547, Tel (800)4BIORAD. Notice regarding Bio-Rad thermal cyclers and real-time systems: Purchase of this instrument conveys a limited non-transferable immunity from suit for the purchaser's own internal research and development and for use in applied fields other than Human In Vitro Diagnostics under one or more of U.S. Patents Nos. 5,656,493, 5,333,675, 5,475,610 (claims 1, 44, 158, 160–163 and 167 only), and 6,703,236 (claims 1–7 only), or corresponding claims in their non-U.S. counterparts, owned by Applied Biosystems Corporation. No right is conveyed expressly, by implication or by estoppel under any other patent claim, such as claims to apparatus, reagents, kits, or methods such as 5' nuclease methods. Further information on purchasing licenses may be obtained by contacting the Director of Licensing, Applied Biosystems, 850 Lincoln Centre Drive, Foster City, California 94404, USA. SYBR is a trademark of Invitrogen Corporation. Bio-Rad Laboratories, Inc. is licensed by Invitrogen Corporation to sell reagents containing SYBR Green I for use in real-time PCR, for research purposes only. Purchase of this product includes an immunity from suit under patents specified in the product insert to use only the amount purchased for the purchaser's own internal research. No other patent rights are conveyed expressly, by implication, or by estoppel. Further information on purchasing licenses may be obtained by contacting the Director of Licensing, Applied Biosystems, 850 Lincoln Centre Drive, Foster City, California 94404, USA.



ELISAs Weighing You Down? Try Bio-Plex.

The new automated Bio-Plex Pro™ wash stations make Bio-Plex assays a more productive alternative.

In a single well, evaluate up to 50 cytokines, chemokines, or growth factors, and use focused disease-related assay panels to better understand:

- Acute phase response
- Cancer
- Diabetes
- Inflammation
- Signal transduction

Run fewer experiments, use less sample, and increase productivity with Bio-Plex multiplex assays.

For more information, go to www.bio-rad.com/bio-plex/



Bio-Plex Pro Assays



Bio-Plex Pro Wash Station

The Bio-Plex suspension array system includes fluorescently labeled microspheres and instrumentation licensed to Bio-Rad Laboratories, Inc. by the Luminex Corporation.

Sample Preparation



Dig Deeper!

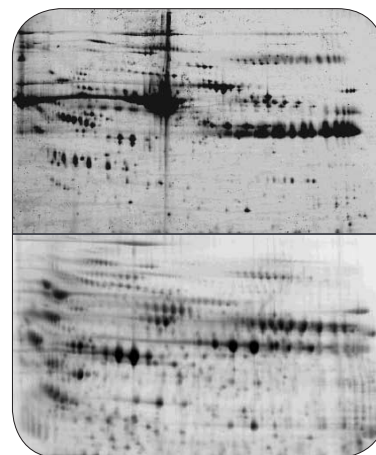
Uncover low-abundance proteins with Bio-Rad's new ProteoMiner™ protein enrichment kits.

ProteoMiner protein enrichment technology is a novel sample preparation tool for reducing the dynamic range of protein concentrations in complex biological samples. The presence of high-abundance proteins in biological samples (for example, albumin and IgG in serum or plasma) makes the detection of low-abundance proteins extremely challenging. ProteoMiner technology presents a method for overcoming this challenge.

- Decrease the amount of high-abundance proteins utilizing a combinatorial library of hexapeptides rather than immunodepletion to prevent co-depletion of low-abundance proteins
- Enrich and concentrate low-abundance proteins that cannot be detected through traditional methods

Whether you use one- or two-dimensional electrophoresis, chromatography, surface-enhanced laser desorption/ionization (SELDI), or another mass spectrometry technique, ProteoMiner kits enable enrichment and detection of low-abundance proteins.

Visit www.bio-rad.com/ad/proteominer/ for more information.



The ProteoMiner protein enrichment kit improves resolution and increases spot counts in two-dimensional gels. Top, untreated plasma; bottom, plasma sample treated with the ProteoMiner kit. Data provided by AstraZeneca.